Molecular basis for the folding of β-helical autotransporter passenger domains

Xiaojun Yuan[1#], Matthew D. Johnson[1#], Jing Zhang[1], Alvin W. Lo[2,3], Mark A. Schembri[2,3], Lakshmi C. Wijeyewickrema[4], Robert N. Pike[4], Gerard H. M. Huysmans[5], Ian R. Henderson[6], and Denisse L. Leyton[1,7]*

1 - Research School of Biology, Australian National University, Canberra, ACT, 0200, Australia

2 - School of Chemistry and Molecular Biosciences, The University of Queensland, Brisbane, Queensland, 4072, Australia

3 - Australian Infectious Disease Research Centre, The University of Queensland, Brisbane, Queensland, 4072, Australia

4 - Department of Biochemistry and Genetics, La Trobe Institute for Molecular Science, La Trobe University, Melbourne, 3086, VIC, Australia

5 - Department of Physiology and Biophysics, Weill Cornell Medicine, New York, NY 10065, U.S.A.

6 - Institute of Microbiology and Infection, University of Birmingham, Birmingham, B15 2TT, UK

7 - Medical School, Australian National University, Canberra, ACT, 0200, Australia

#These authors contributed equally to this work

*To whom correspondence should be addressed: denisse.leyton@anu.edu.au

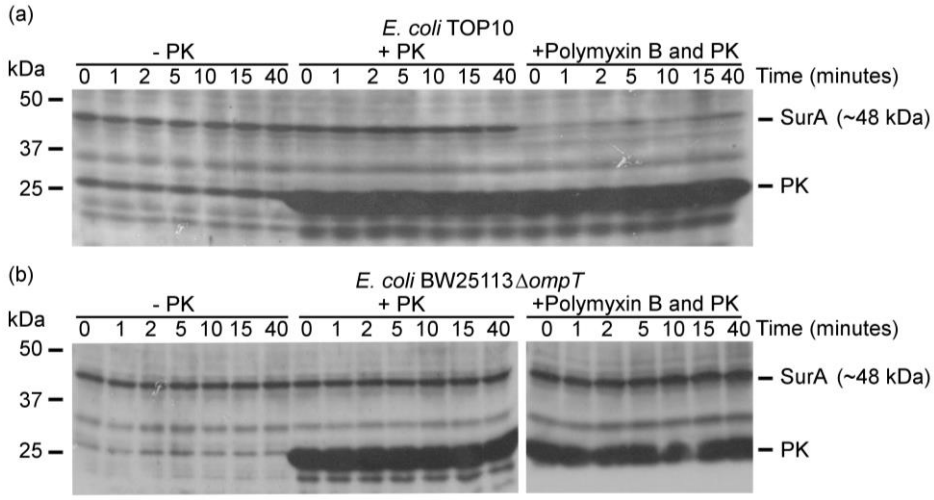

Supplementary Figure 1 | Proteinase K does not permeabilize the outer membrane of *E. coli* TOP10 or *E. coli* BW25113Δ*ompT*. (a) *E. coli* TOP10 and **(b)** *E. coli* BW25113Δ*ompT* incubated for up to 40 min of a mock 'chase' period at 25 °C and then immediately precipitated with TCA (- PK), or incubated on ice with 200 mg/mL proteinase K (+ PK), or incubated on ice with 200 mg/mL polymyxin B and 200 mg/mL proteinase K (+ Polymyxin B and PK). After addition of Phenylmethanesulfonyl fluoride (see Methods), proteinase K-treated samples were TCA precipitated and all samples were then analyzed by SDS-PAGE and immunoblotting for the periplasmic protein SurA. In both bacterial strains, the intact SurA protein (48 kDa) was observed in – PK and + PK samples. Note that a thick band corresponding to the migration position of proteinase K is also observed. These data show that the amount of proteinase K in use does not permeabilize the *E. coli* outer membrane, which remains intact during proteinase K treatment. Furthermore, SurA was degraded almost to completion by proteinase K in the presence of polymyxin B in *E. coli* TOP10. In contrast, intact SurA was observed in samples treated with proteinase K in the presence of polymyxin B in *E. coli* BW25113Δ*ompT*, indicating that 200 mg/mL polymyxin B is insufficient to permeabilize this strain's outer membrane. As a consequence, only *E. coli* TOP10 was used to perform pulse-chase assays in the presence of polymyxin B and proteinase K in this study. Images are representative of at least two independent experiments.

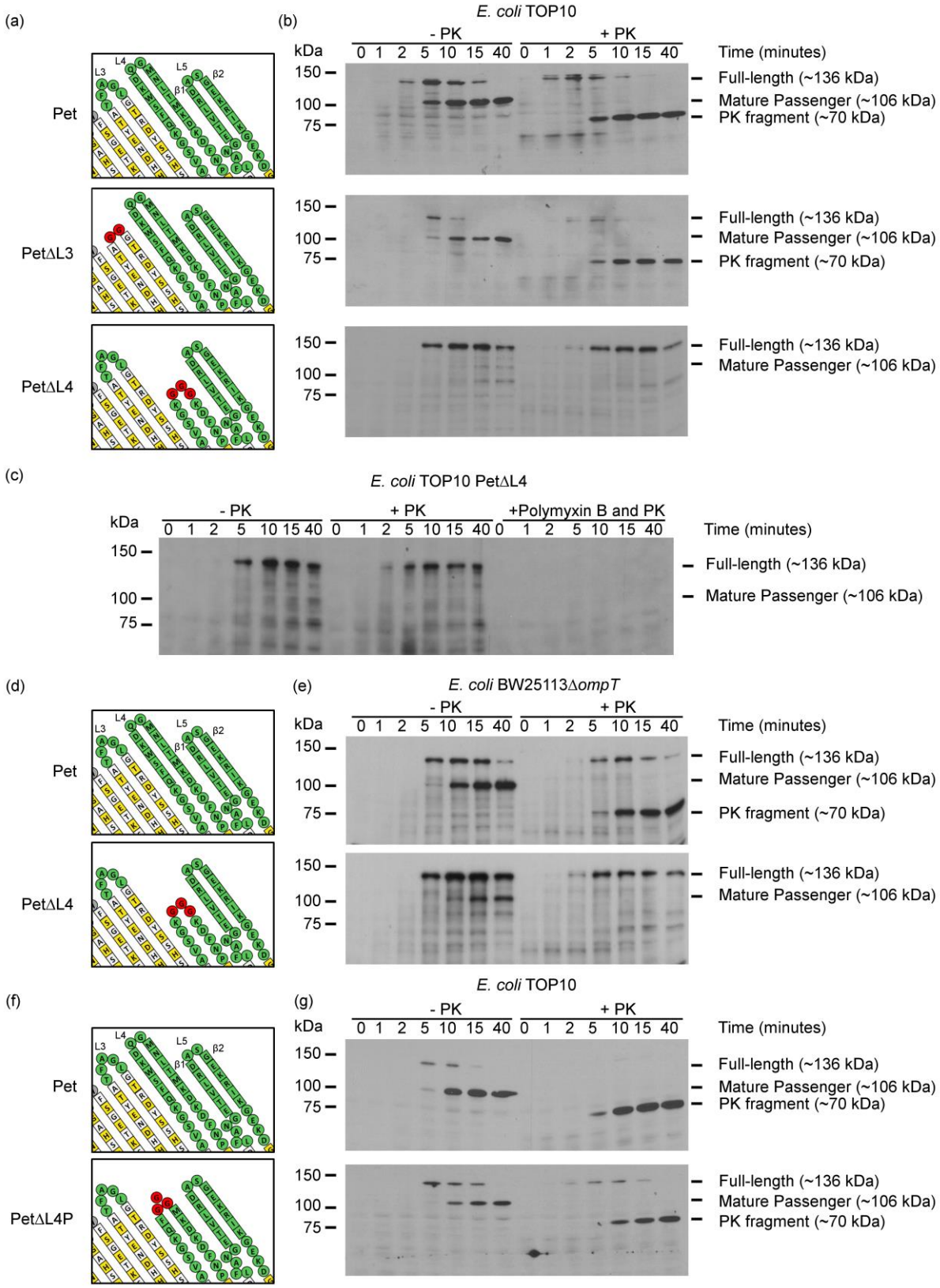
(a)
(b)
E. coli TOP10
- PK
+ PK
kDa
0 1 2 5 10 15 40 0 1 2 5 10 15 40
Time (minutes)
150
100
75
Pet
PetΔL3
PetΔL4
Full-length (~136 kDa)
Mature Passenger (~106 kDa)
PK fragment (~70 kDa)
(c)
E. coli TOP10 PetΔL4
+Polymyxin B and PK
0 1 2 5 10 15 40 0 1 2 5 10 15 40 0 1 2 5 10 15 40
(d)
(e)
E. coli BW25113ΔompT
PetΔL4P
(f)
(g)
L3
L4
L5
β1
β2

Supplementary Figure 2 | Truncation of L4 perturbs passenger domain translocation. (a) Topology model of the Pet β-barrel domain showing the L3 and L4 truncations created by replacing T_{1130}-L_{1134} and Q_{1177}-D_{1191} with two and with three glycine residues (shown in red), respectively. **(b)** Pulse-chase expression of Pet, PetΔL3 and PetΔL4, and sensitivity to proteinase K (PK) in *E. coli* TOP10. **(c)** Pulse-chase PetΔL4 maturation as above, but also in the presence of polymyxin B prior to the addition of proteinase K as indicated (+ Polymyxin B and PK). **(d)** Topology model of the Pet β-barrel domain showing the L4 truncation created by replacing Q_{1177}-D_{1191} with three glycine residues (shown in red). **(e)** Pulse-chase expression of Pet and PetΔL4, and sensitivity to proteinase K (PK) in *E. coli* BW25113Δ*ompT*. **(f)** Topology model of the Pet β-barrel domain showing the partial L4 truncation created by replacing S_{1179}-T_{1188} with three glycine residues (shown in red). **(g)** Pulse-chase expression of Pet and PetΔL4P, and sensitivity to proteinase K (PK) in *E. coli* TOP10. All samples were TCA precipitated prior to SDS-PAGE and immunoblotting with anti-Pet passenger domain antibodies. Images are representative of at least two independent experiments.

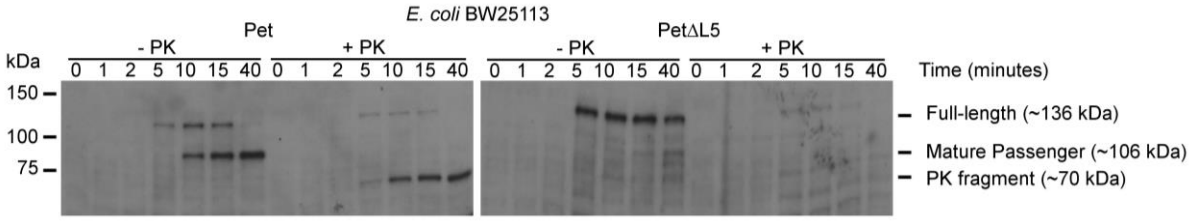

Supplementary Figure 3 | Pet biogenesis in *E. coli* BW25113. Pulse-chase expression of Pet and PetΔL5, and sensitivity to proteinase K (PK) in *E. coli* BW25113 monitored by SDS-PAGE and immunoblotting with anti-Pet passenger domain antibodies. All samples were TCA precipitated prior to SDS-PAGE. Image is representative of at least two independent experiments.

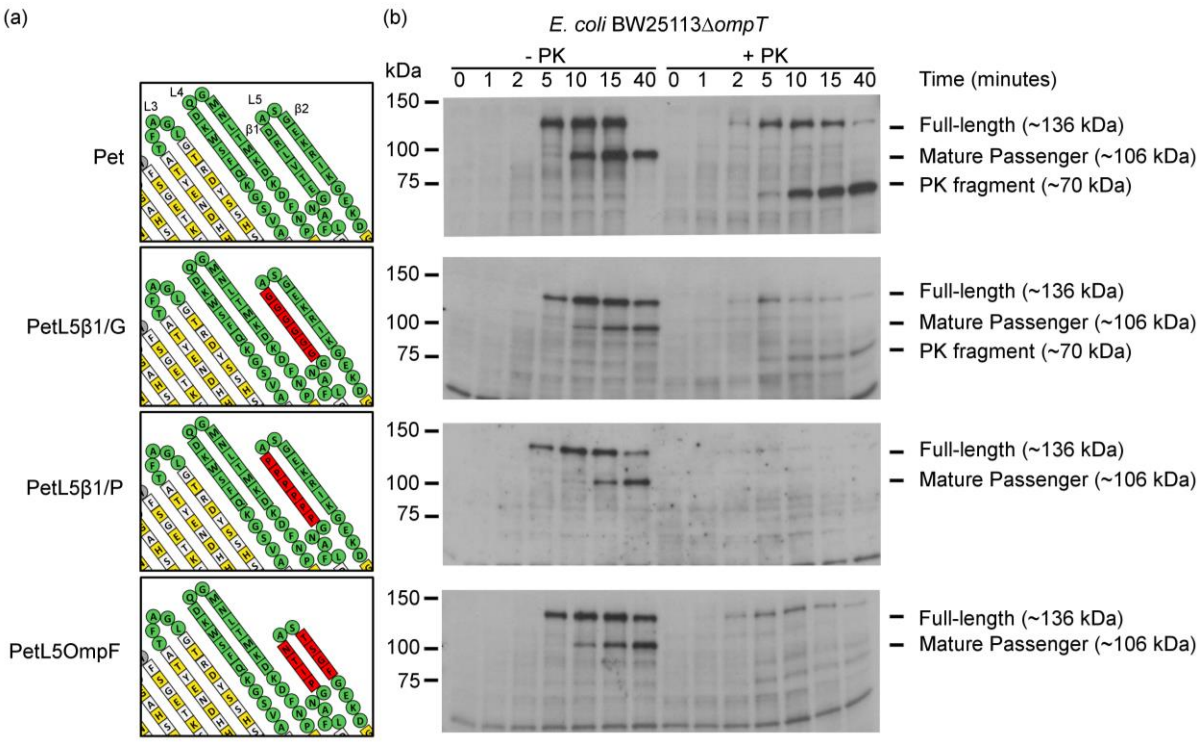

Supplementary Figure 4 | Mutation of L5 affects folding of the Pet passenger domain. (a) Topology model of the Pet β-barrel domain showing the $Pet^{L5\beta1/G}$, $Pet^{L5\beta1/P}$ and Pet^{L5OmpF} mutations (in red). **(b)** Pulse-chase expression of Pet, $Pet^{L5\beta1/G}$, $Pet^{L5\beta1/P}$ and Pet^{L5OmpF}, and sensitivity to proteinase K (PK) in *E. coli* BW25113Δ*ompT* monitored by SDS-PAGE and immunoblotting with anti-Pet passenger domain antibodies. All samples were TCA precipitated prior to SDS-PAGE. Images are representative of at least two independent experiments.

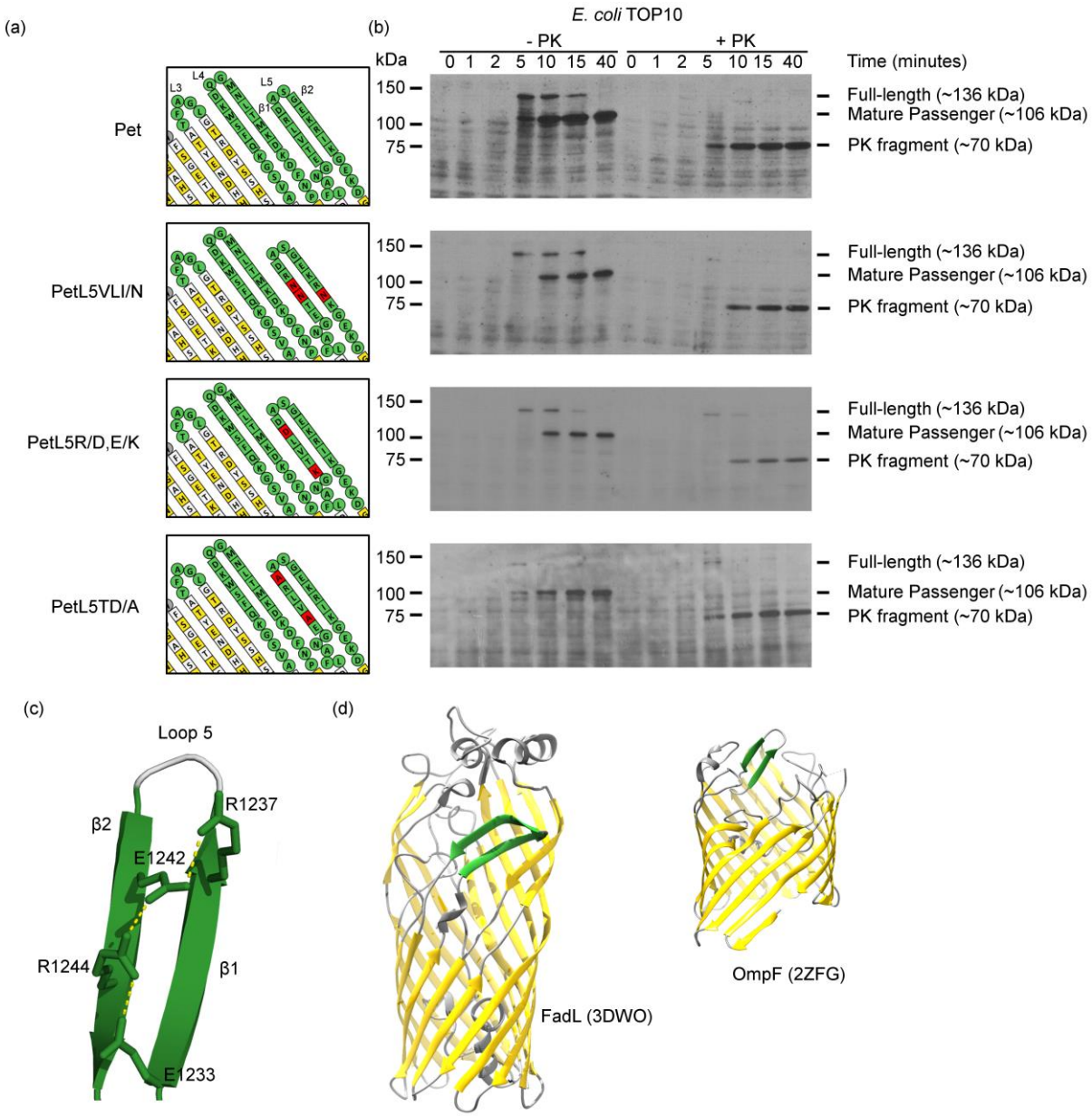

Supplementary Figure 5 | Hydrophobic and charged residues do not mediate passenger folding. (a) Topology model of the Pet β-barrel domain showing the $Pet^{L5VLI/N}$, $Pet^{L5R/D,E/K}$ and $Pet^{L5TD/A}$ mutations (in red). **(b)** Pulse-chase expression of Pet, $Pet^{L5VLI/N}$, $Pet^{L5R/D,E/K}$ and $Pet^{L5TD/A}$, and sensitivity to proteinase K (PK) in *E. coli* TOP10 monitored by SDS-PAGE and immunoblotting with anti-Pet passenger domain antibodies. All samples were TCA precipitated prior to SDS-PAGE. Images are representative of at least two independent experiments. **(c)** The crystal structure of the EspP β-barrel domain (PDB code 3SLJ) showing putative salt-bridge interactions between R_{1237} in β-strand 1 and E_{1242} in β-strand 2 (top of L5), and a E_{1233} in β-strand 1 and R_{1244} in β-strand 2 (bottom of L5). **(d)** The crystal structures of FadL from *Pseudomonas aeruginosa* (PDB code 3DWO) and OmpF from *E. coli* (PDB code 2ZFG). In each case, the β-strands within the β-hairpin loop are shown in green.

(a)

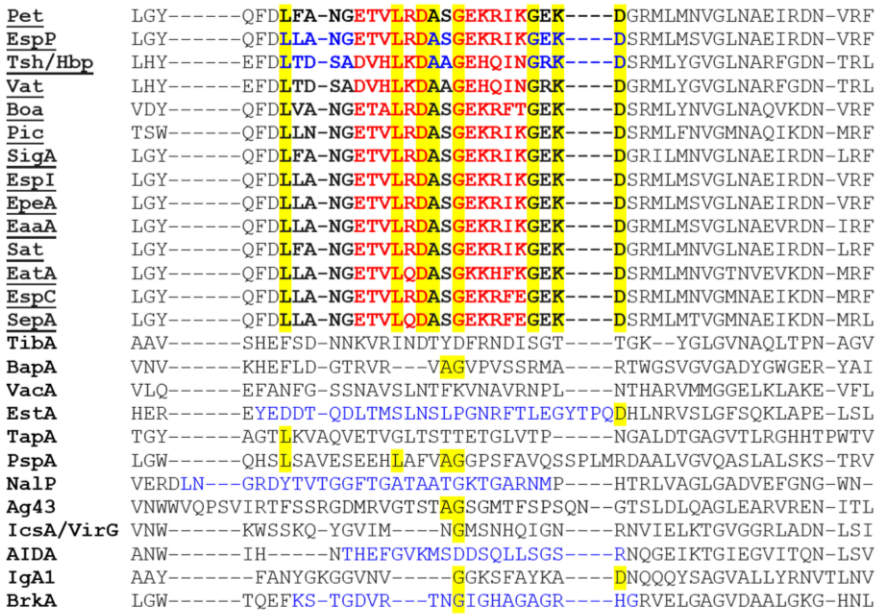

(b)

			Tsh/Hbp	Vat	Boa	Pic	SigA	EspI	EspP	EpeA	EaaA	Sat	Pet	EatA	EspC	SepA
			1	2	3	4	5	6	7	8	9	10	11	12	13	14
Tsh/Hbp	1	(Type_5)	100.0	98.92	62.09	62.45	60.65	61.01	61.73	62.09	62.45	62.09	62.45	59.21	62.09	61.01
Vat	2	(Type_5)	98.92	100.0	61.37	62.45	61.37	60.65	61.37	61.73	62.82	62.45	62.82	59.21	62.09	61.01
Boa	3	(Type_5)	62.09	61.37	100.0	71.84	68.59	68.59	69.68	69.68	68.59	68.23	68.95	64.98	70.04	67.15
Pic	4	(Type_5)	62.45	62.45	71.84	100.0	79.06	80.14	80.14	80.14	80.87	79.06	79.78	71.48	79.42	77.26
SigA	5	(Type_5)	60.65	61.37	68.59	79.06	100.0	86.28	87.73	87.36	88.09	88.81	89.17	71.84	81.23	78.70
EspI	6	(Type_5)	61.01	60.65	68.59	80.14	86.28	100.0	96.75	96.39	90.97	88.81	89.89	72.56	79.42	77.26
EspP	7	(Type_5)	61.73	61.37	69.68	80.14	87.73	96.75	100.0	99.64	92.42	89.89	90.97	73.65	81.23	79.06
EpeA	8	(Type_5)	62.09	61.73	69.68	80.14	87.36	96.39	99.64	100.0	92.78	90.25	91.34	73.65	81.59	79.42
EaaA	9	(Type_5)	62.45	62.82	68.59	80.87	88.09	90.97	92.42	92.78	100.0	92.42	93.14	74.37	81.95	79.42
Sat	10	(Type_5)	62.09	62.45	68.23	79.06	88.81	88.81	89.89	90.25	92.42	100.0	98.92	72.92	80.14	77.98
Pet	11	(Type_5)	62.45	62.82	68.95	79.78	89.17	89.89	90.97	91.34	93.14	98.92	100.0	73.65	80.87	78.70
EatA	12	(Type_5)	59.21	59.21	64.98	71.48	71.84	72.56	73.65	73.65	74.37	72.92	73.65	100.0	83.39	80.87
EspC	13	(Type_5)	62.09	62.09	70.04	79.42	81.23	79.42	81.23	81.59	81.95	80.14	80.87	83.39	100.0	94.22
SepA	14	(Type_5)	61.01	61.01	67.15	77.26	78.70	77.26	79.06	79.42	79.42	77.98	78.70	80.87	94.22	100.0

(c)

			EstA	VacA	NalP	Ag43	TapA	PspA	IgA1	IcsA/VirG	AIDA	BrkA	TibA/TynE	BapA
			1	2	3	4	5	6	7	8	9	10	11	12
EstA	1	(Type_4)	100.0	15.30	16.01	12.78	14.03	18.73	12.88	16.30	15.99	14.49	13.62	14.03
VacA	2	(Type_3)	15.30	100.0	11.66	15.65	13.26	16.73	15.13	15.30	14.55	15.90	15.79	11.64
NalP	3	(Type_6)	16.01	11.66	100.0	13.74	15.27	17.73	16.04	13.11	13.86	16.30	15.30	13.98
Ag43	4	(Type_13)	12.78	15.65	13.74	100.0	14.06	15.47	14.46	17.10	15.30	20.15	19.62	19.62
TapA	5	(Type_2)	14.03	13.26	15.27	14.06	100.0	19.00	15.06	12.36	14.29	16.48	13.55	12.88
PspA	6	(Type_1)	18.73	16.73	17.73	15.47	19.00	100.0	16.79	19.03	16.04	20.30	16.79	17.52
IgA1	7	(Type_8)	12.88	15.13	16.04	14.46	15.06	16.79	100.0	17.18	15.65	17.75	24.01	15.93
IcsA/VirG	8	(Type_12)	16.30	15.30	13.11	17.10	12.36	19.03	17.18	100.0	37.46	18.08	20.37	18.51
AIDA	9	(Type_13)	15.99	14.55	13.86	15.30	14.29	16.04	15.65	37.46	100.0	17.34	20.74	17.08
BrkA	10	(Type_10)	14.49	15.90	16.30	20.15	16.48	20.30	17.75	18.08	17.34	100.0	26.37	21.00
TibA/TynE	11	(Type_10)	13.62	15.79	15.30	19.62	13.55	16.79	24.01	20.37	20.74	26.37	100.0	21.75
BapA	12	(Type_14)	14.03	11.64	13.98	19.62	12.88	17.52	15.93	18.51	17.08	21.00	21.75	100.0

Supplementary Figure 6 | Multiple sequence alignment and percent identity of autotransporter β-barrel domains. (a) Multiple sequence alignment (performed using Muscle[1]) on the amino acid sequence of β-barrel domains that are representative of 11 distinct Types. The residues corresponding to L5 of EspP (PDB 3SLJ), Tsh/Hbp (PDB 3AEH), EstA (PDB 3KVN), AIDA-I (PDB 4MEE), NalP (PDB 1UYN), and BrkA (PDB 3QQ2) are shown in blue font and mapped according to their crystal structures. The L5 regions in SPATE β-barrels (shown in black font and underlined) are the same length and contain several residues that are highly or completely conserved (highlighted in yellow), particularly within the regions that form a β-hairpin (shown in red font). The L5 regions in non-SPATE β-barrel domains (shown in black font) differ substantially with each other and with those in SPATEs. **(b)** Percent identity between SPATE β-barrel domains ranges from 59.21- to- 99.64 %. **(c)** Percent identity between non-SPATE β-barrel domains ranges from 11.64- to- 37.46 % and even those belonging to the same Type share low sequence identity.

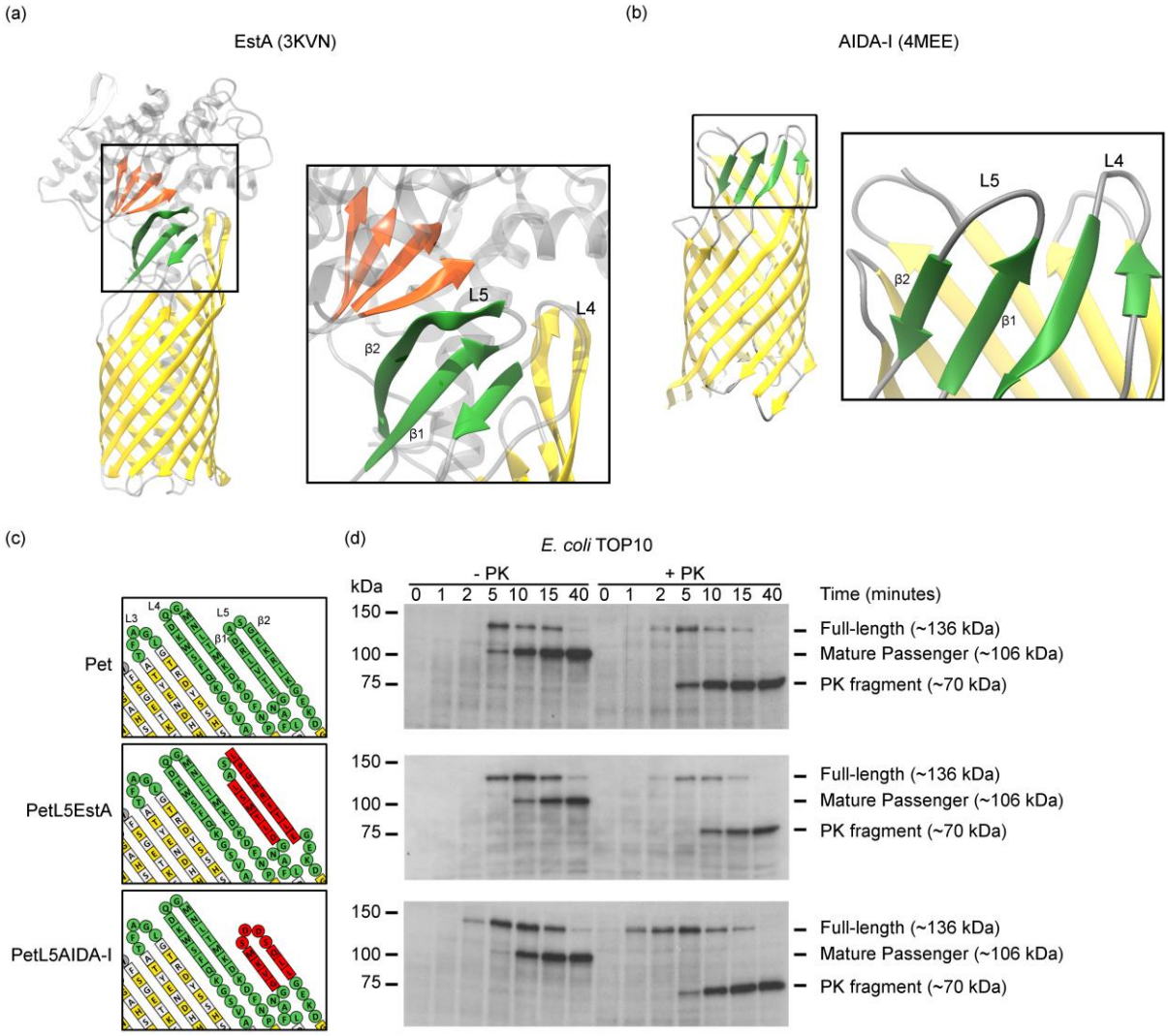

Supplementary Figure 7 | Structural analysis of the AIDA-I and EstA β-barrel domains. The crystal structures of EstA from *P. aeruginosa* (PDB code 3KVN) **(a)** and AIDA-I from *E. coli* (PDB code 4MEE) **(b)**. In each case, the β-strands within the L5 and L4 β-hairpins are shown in green. The central four-stranded parallel β-sheet within the globular passenger domain of EstA is shown in orange. **(c)** Topology model of the Pet β-barrel domain showing the Pet^{L5EstA} and $Pet^{L5AIDA-I}$ mutations (in red). **(d)** Pulse-chase expression of Pet^{L5EstA} and $Pet^{L5AIDA-I}$, and sensitivity to proteinase K (PK) in *E. coli* TOP10 monitored by SDS-PAGE and immunoblotting with anti-Pet passenger domain antibodies. All samples were TCA precipitated prior to SDS-PAGE. Images are representative of at least two independent experiments.

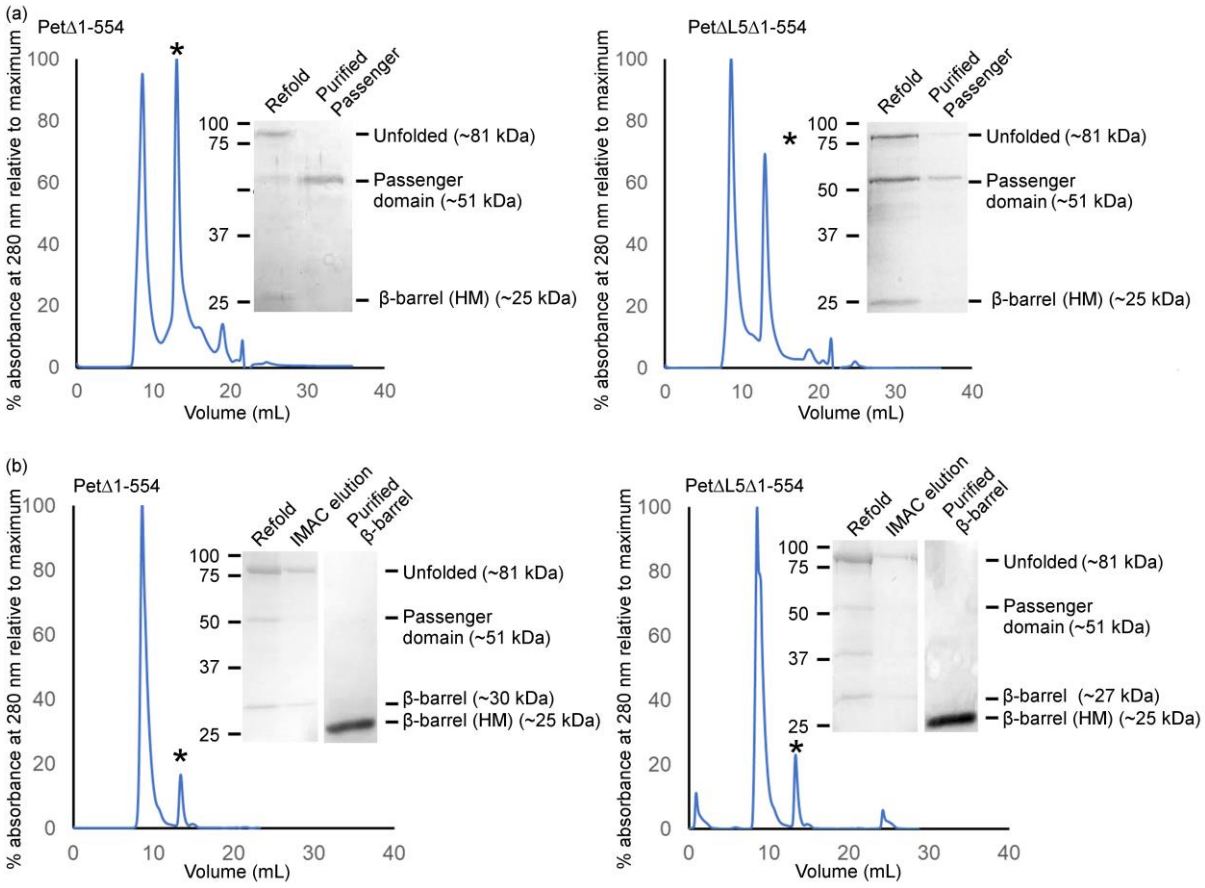

Supplementary Figure 8 | Purification of Pet$^{\Delta 1\text{-}554}$ and PetΔL5$^{\Delta 1\text{-}554}$. (a) Cleaved passenger domains were purified further by gel filtration in LDAO free buffer (* indicates the passenger domain elution peak), resulting in a batch of protein containing just the ~51 kDa species as analysed by SDS-PAGE and Coomassie staining (insets). **(b)** Cleaved β-barrel domains were purified further by gel filtration chromatography in buffer containing 0.05% (w/v) LDAO (* indicates the β-barrel elution peak), resulting in a batch of protein containing just the cleaved ~30 kDa species as analysed by SDS-PAGE and Coomassie staining (inset). Heat modifiability (HM) in the *in vitro*-folded Pet$^{\Delta 1\text{-}554}$ and PetΔL5$^{\Delta 1\text{-}554}$ β-barrels was evident by the increased migration of the folded species from samples exposed to SDS at 25 °C.

Figure 1e Pet

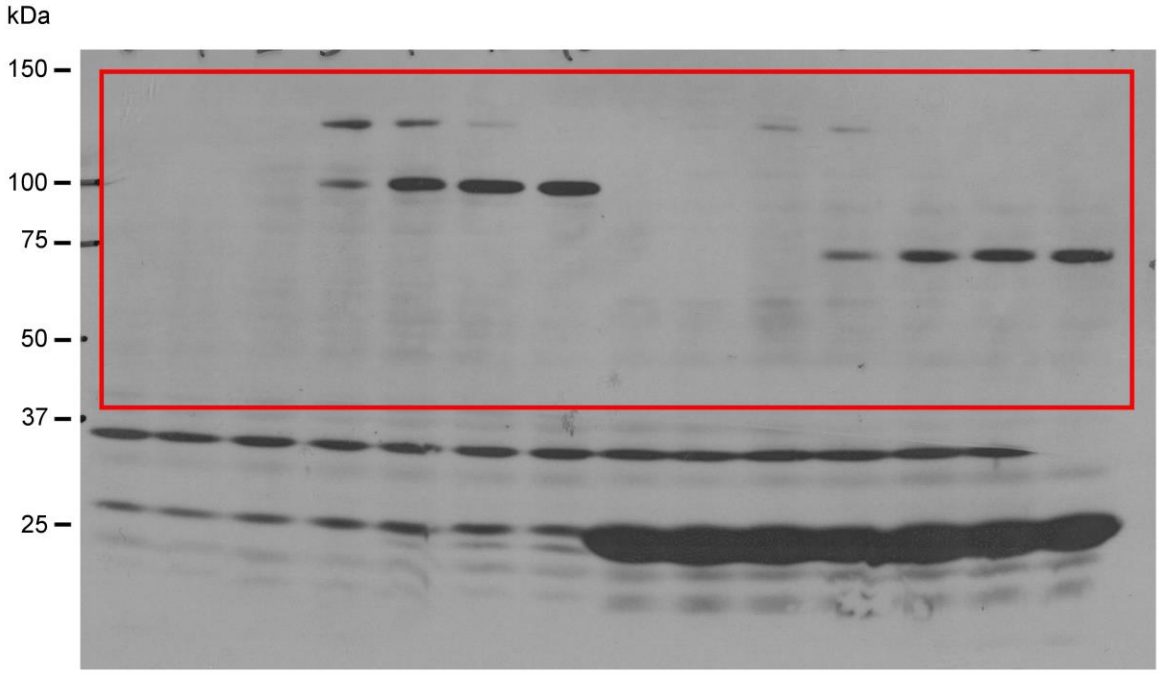

Figure 1e PetΔL5

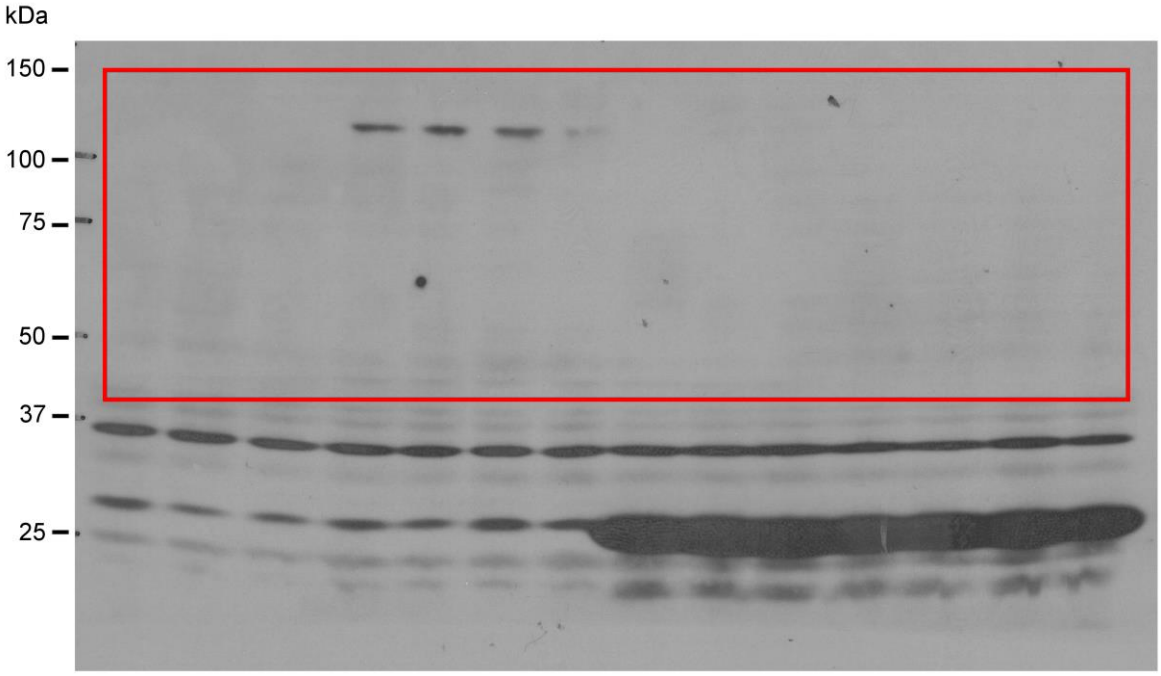

Figure 1f Pet

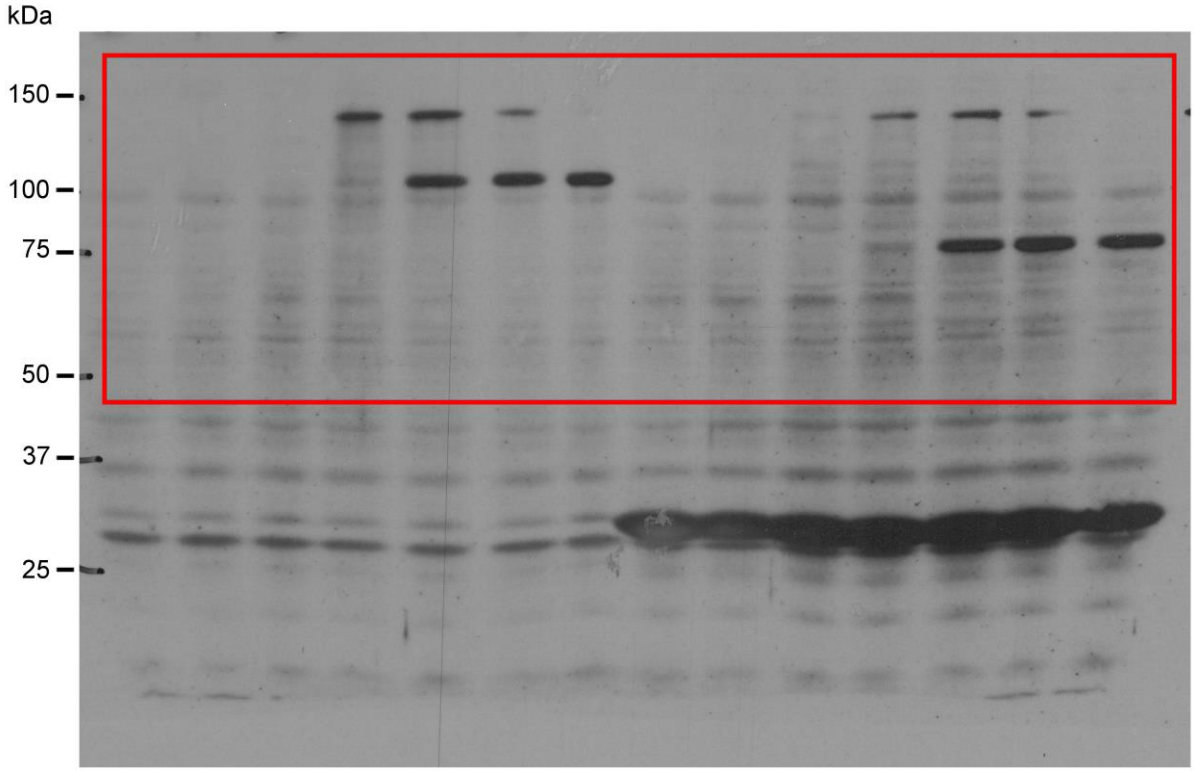

Figure 1f PetΔL5

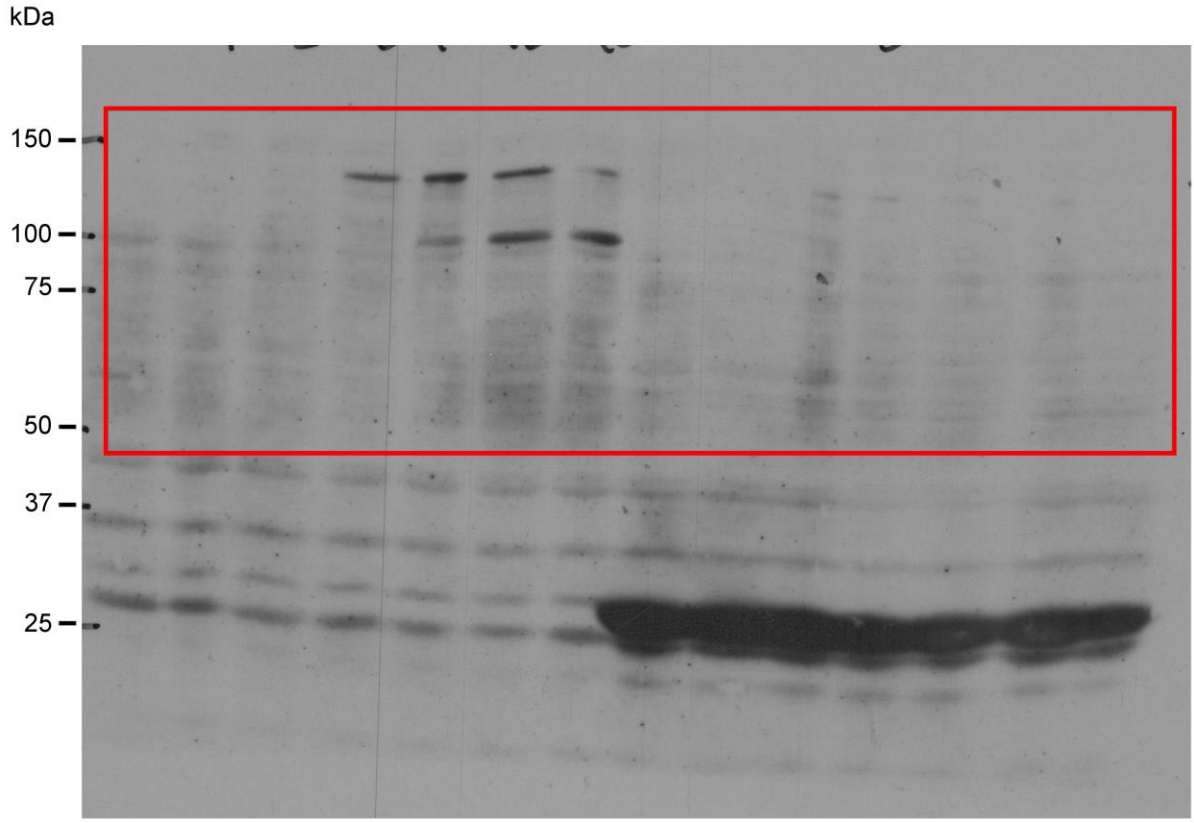

Figure 1g

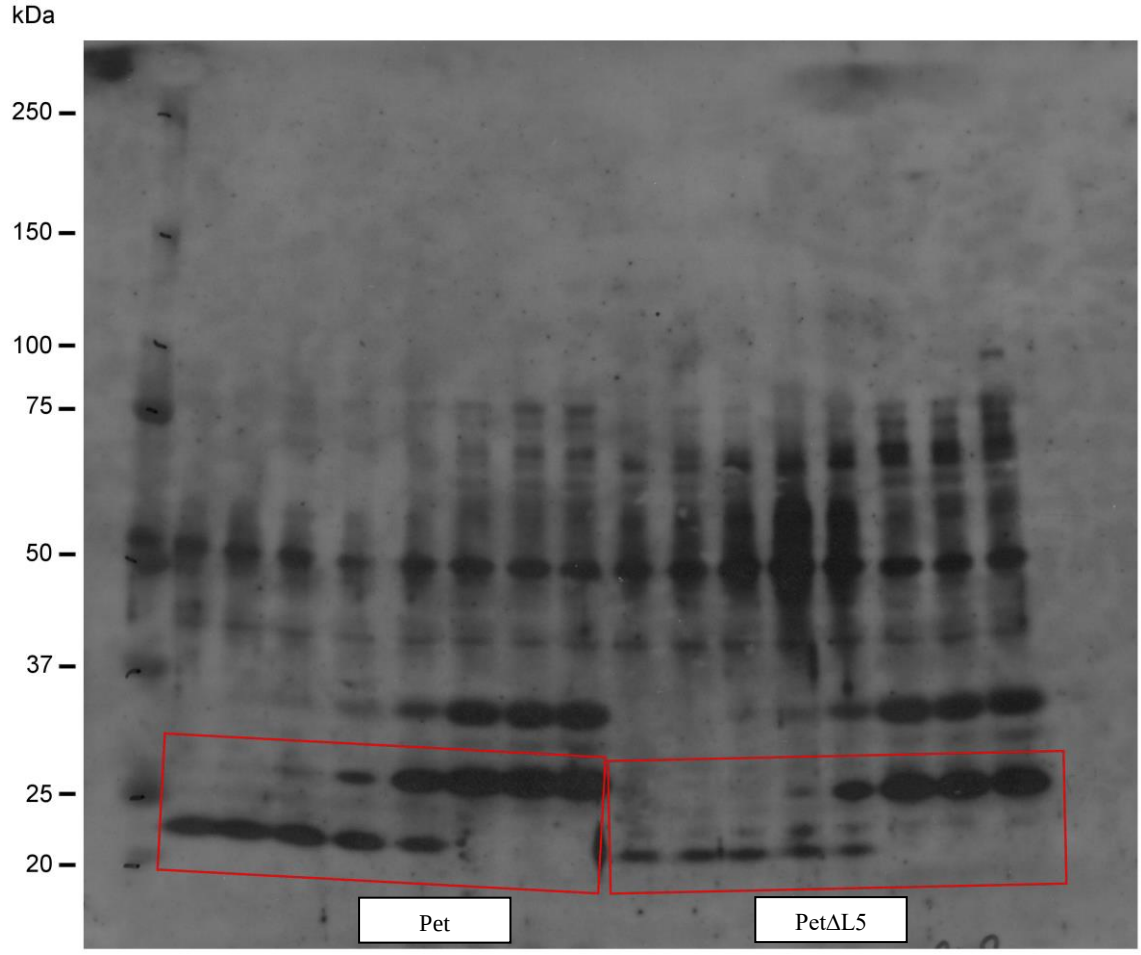

Figure 2c Pet

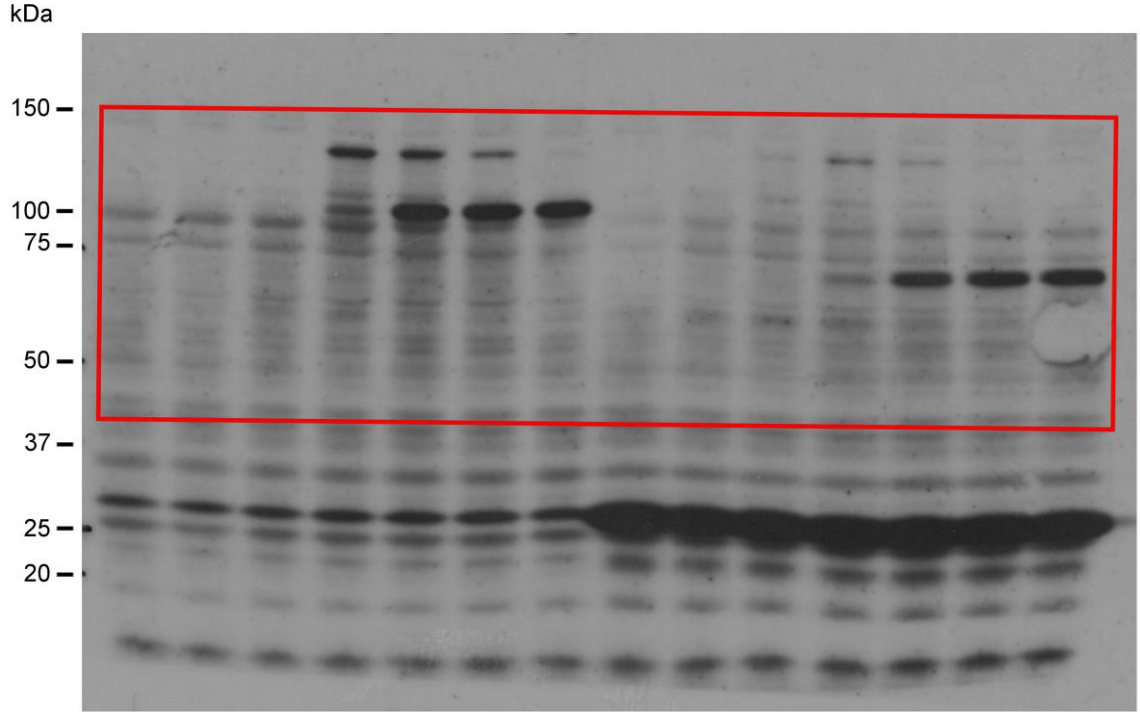

Figure 2c PetL5β1/G

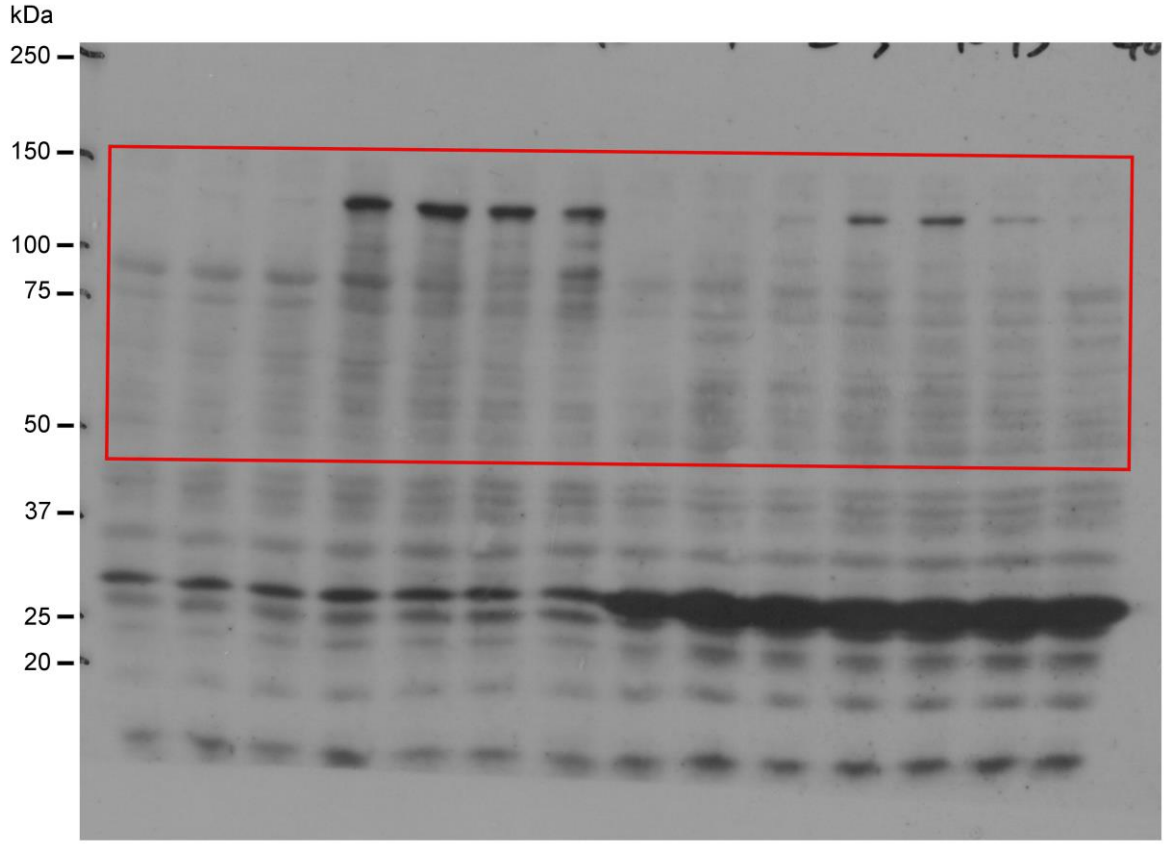

Figure 2c PetL5β2/G

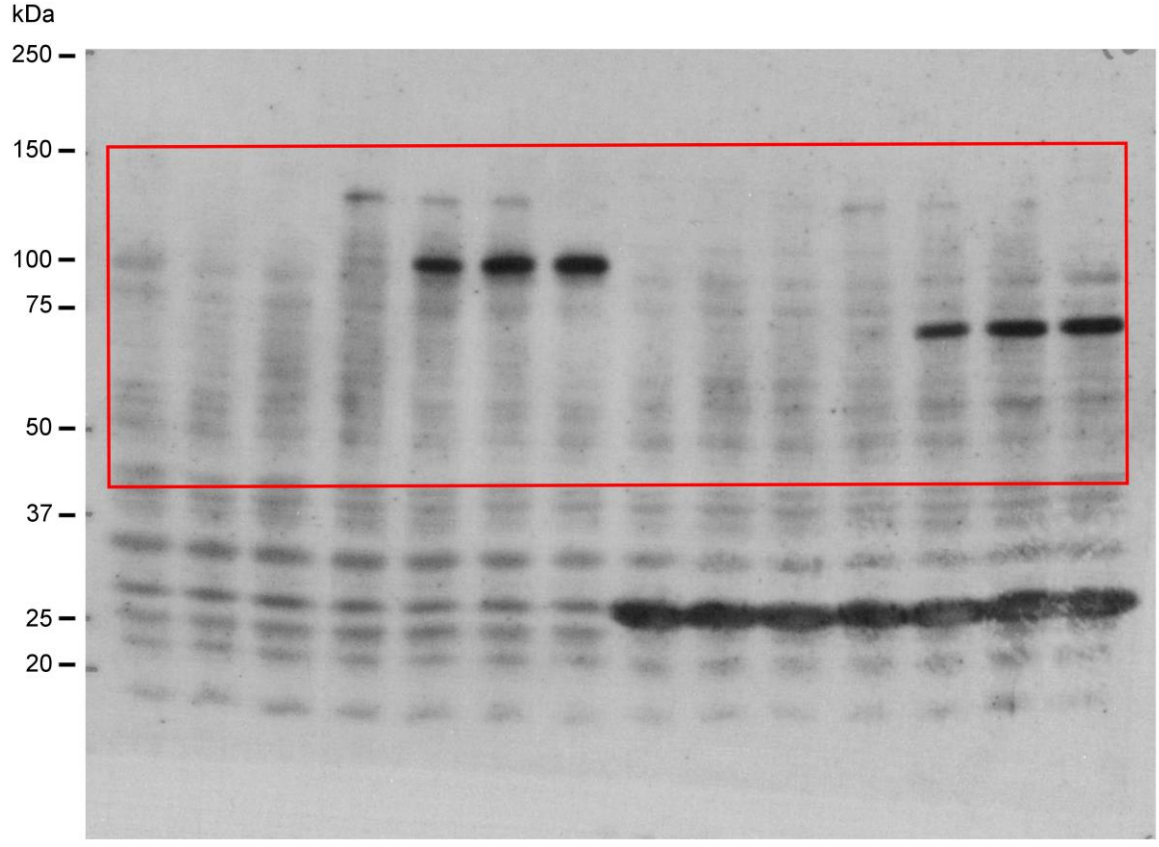

Figure 2c PetL5Un/G

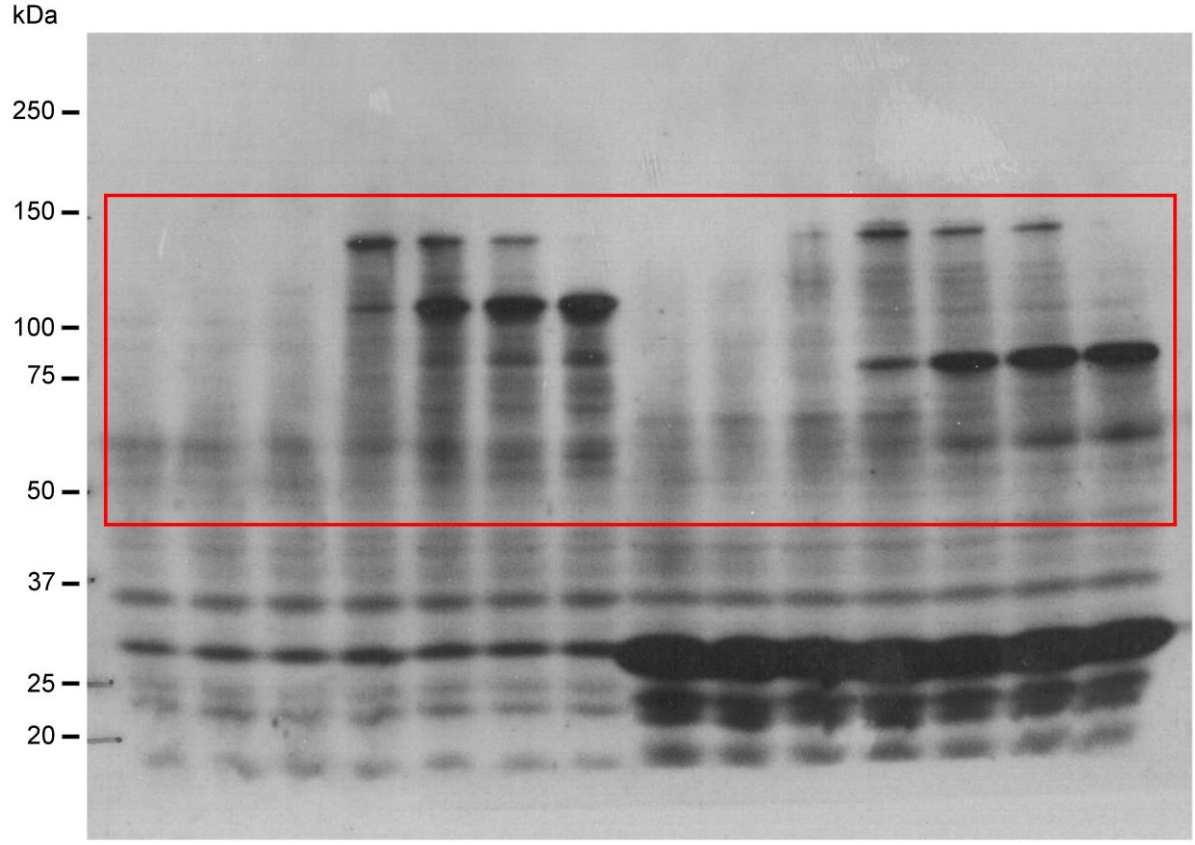

Figure 2d Pet

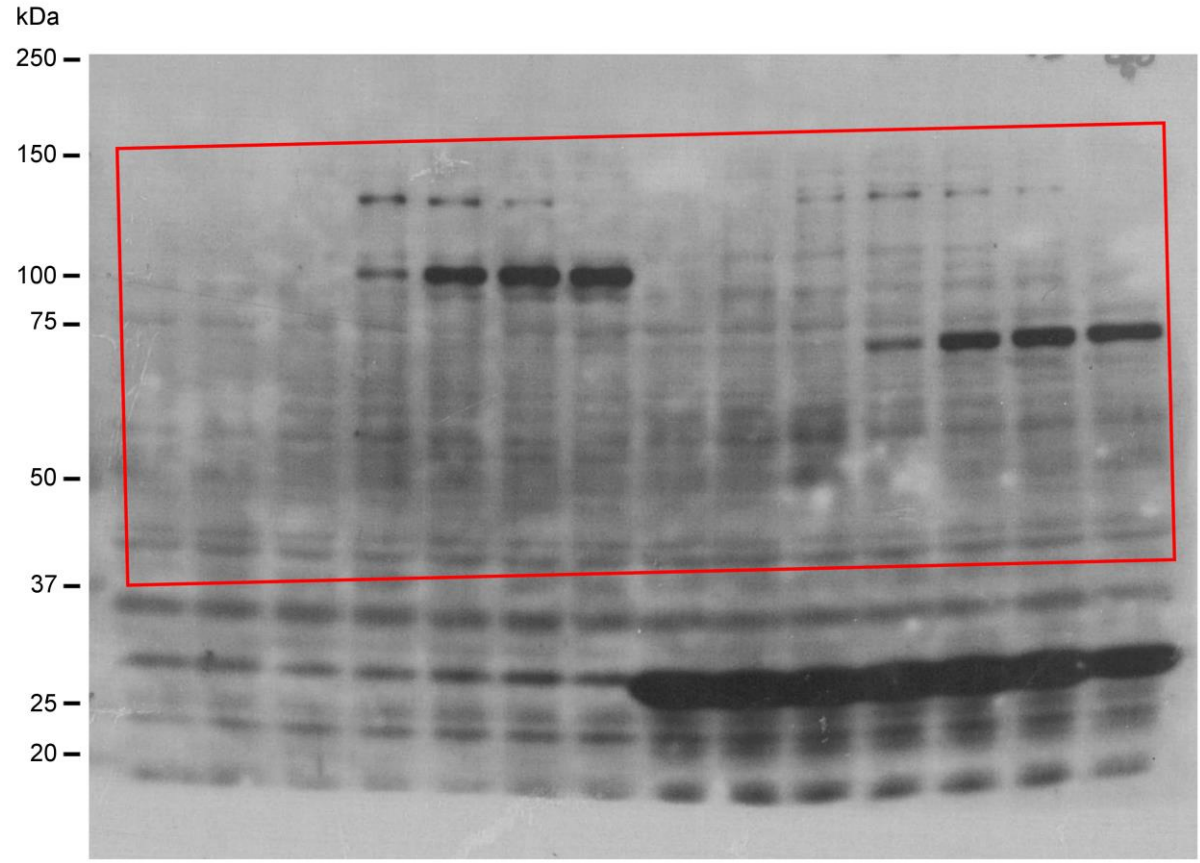

Figure 2d PetL5OmpF

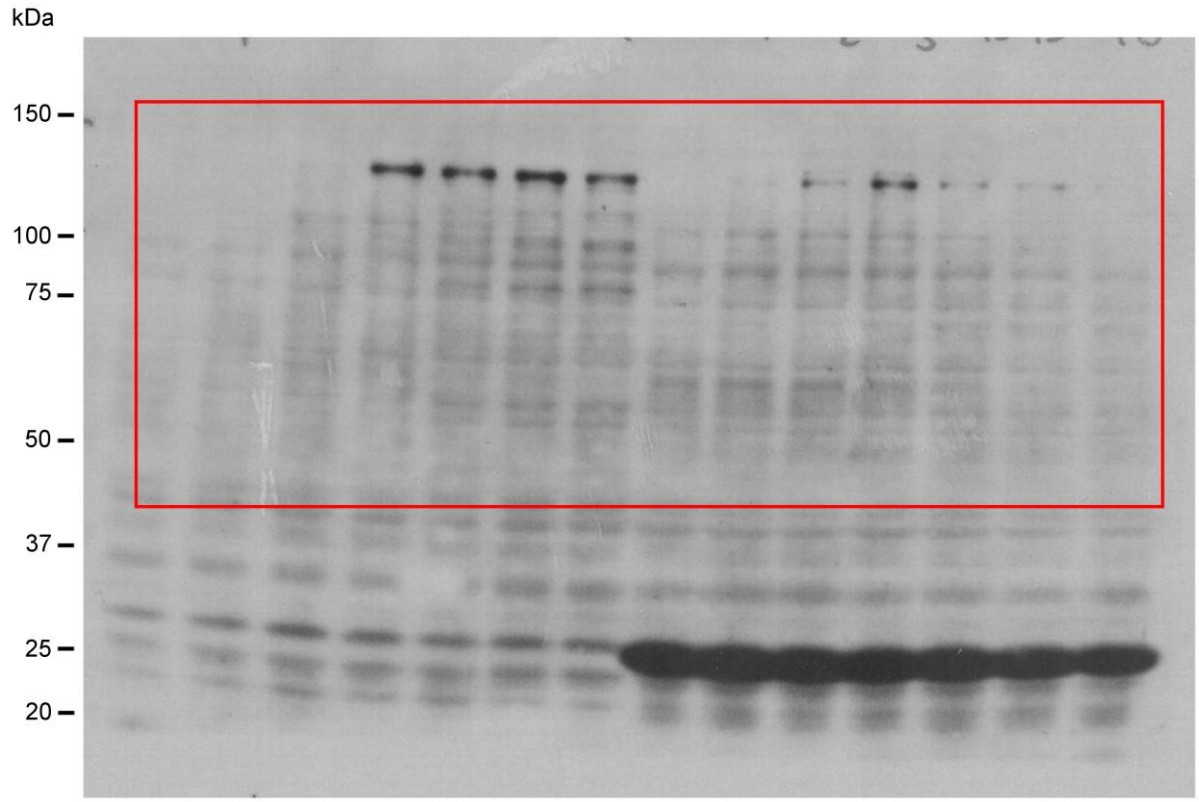

Figure 2d PetL5FadL

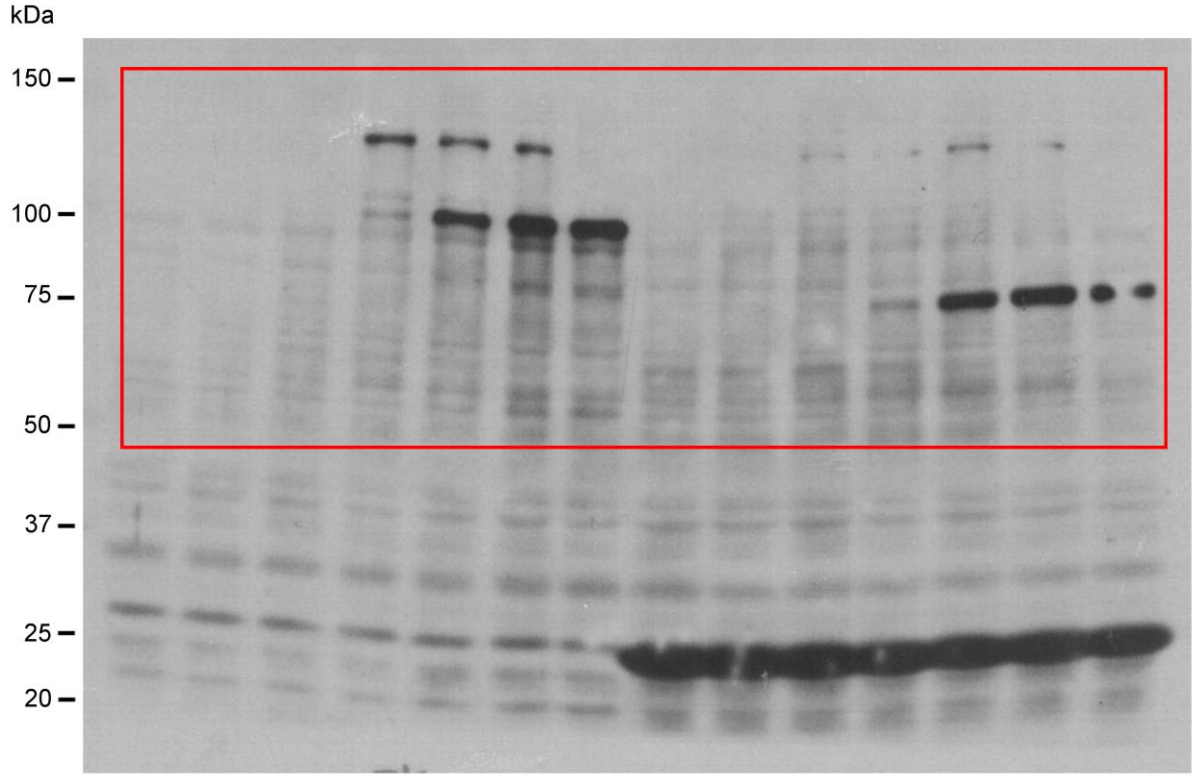

Figure 2d PetL5β1/P

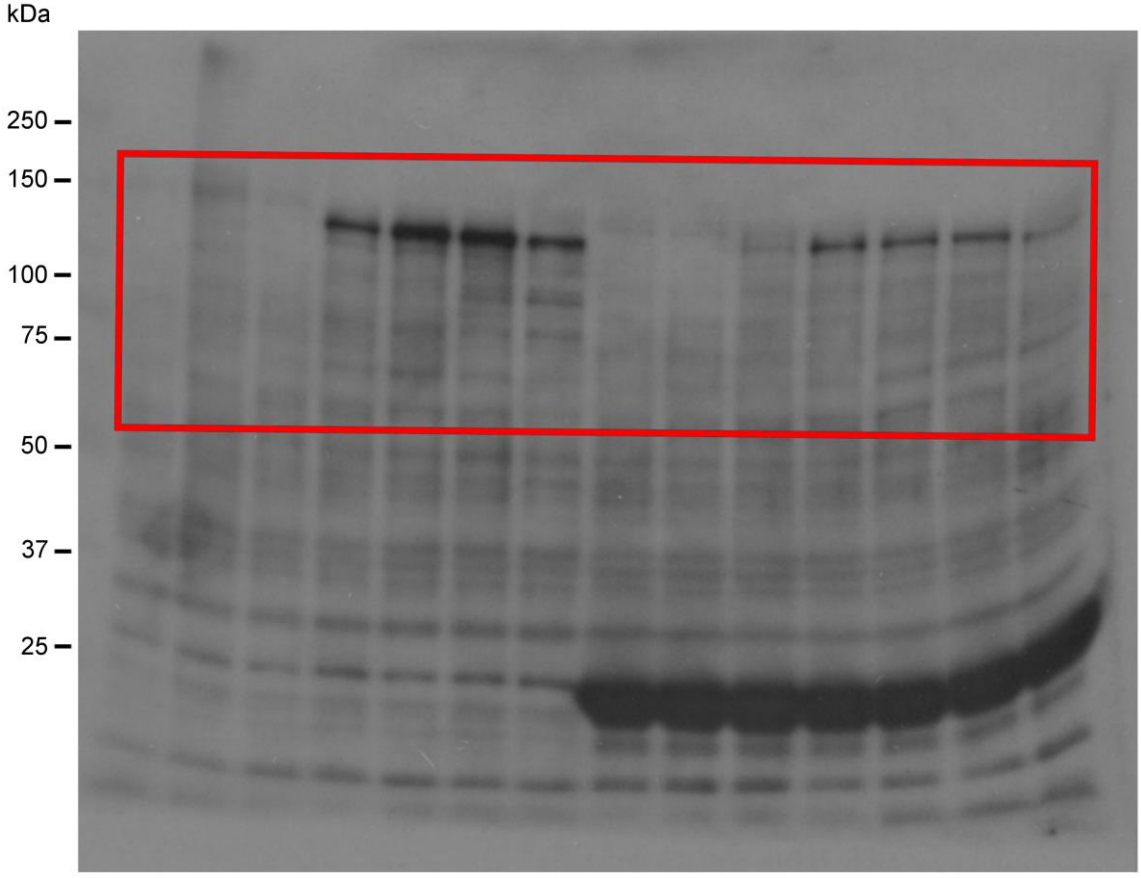

Figure 3b top

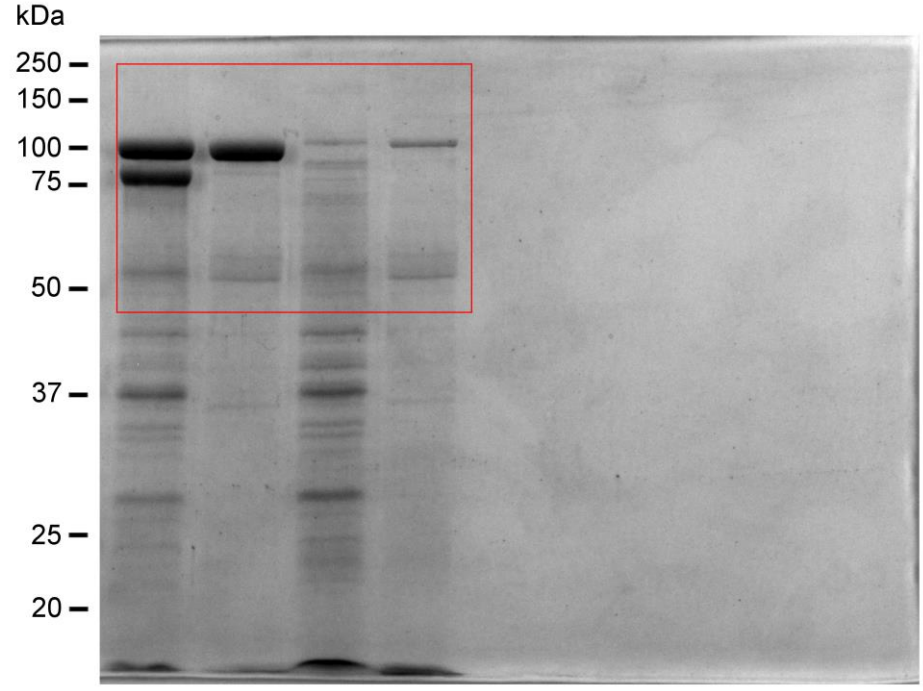

Figure 3b bottom

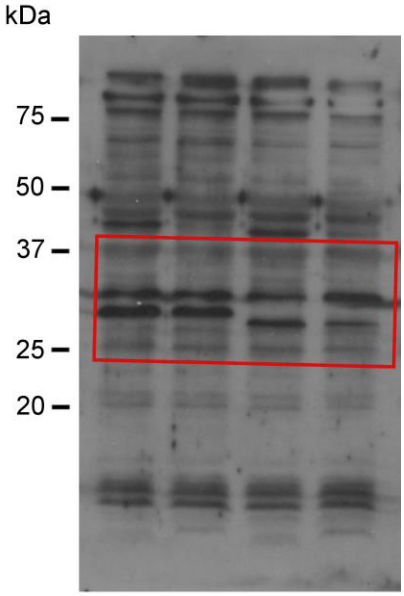

Figure 4b

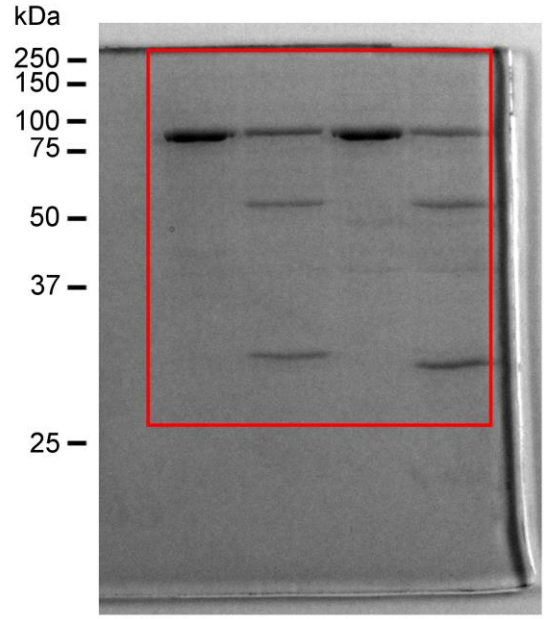

Figure 4c Passenger antibody (top)

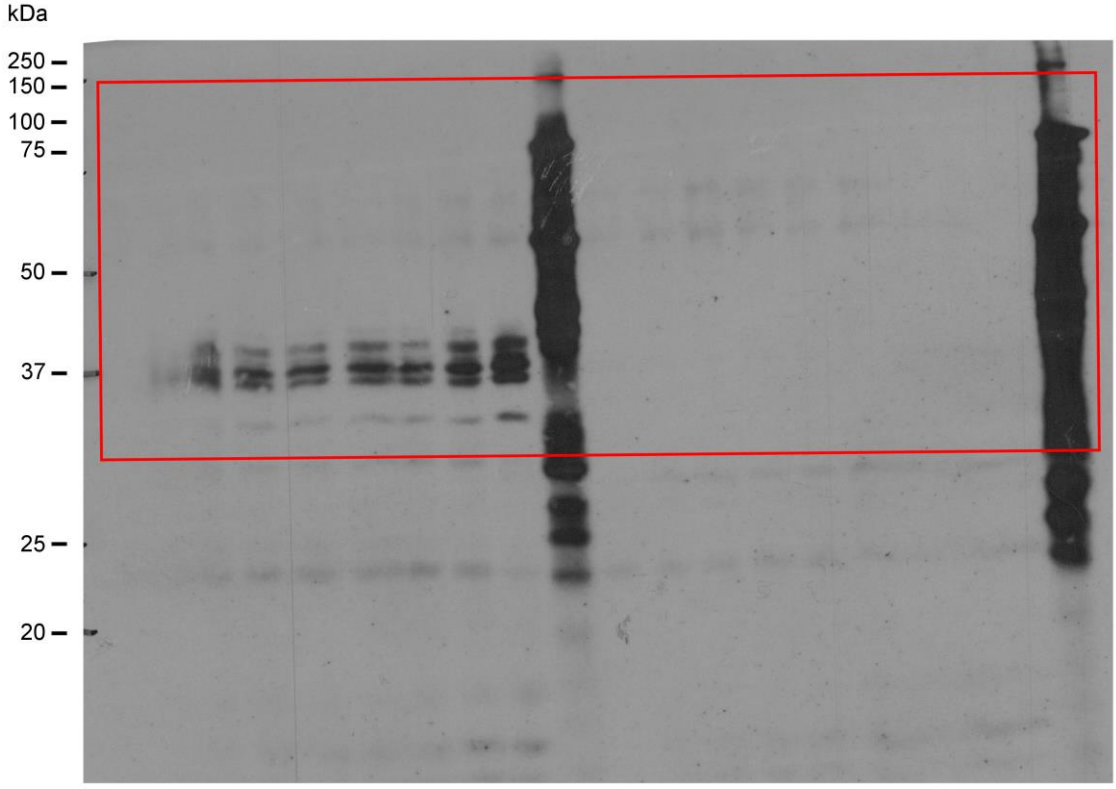

Figure 4c β-barrel antibody (bottom)

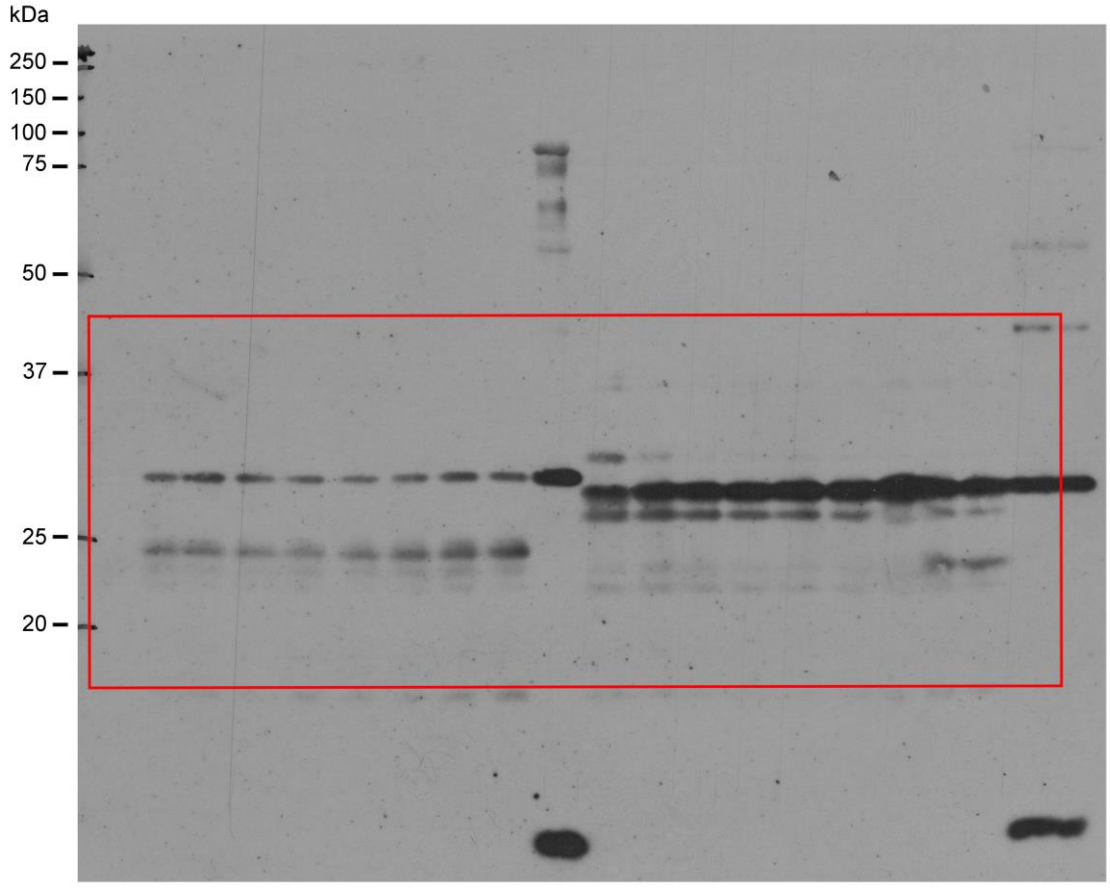

Supplementary Figure 1a

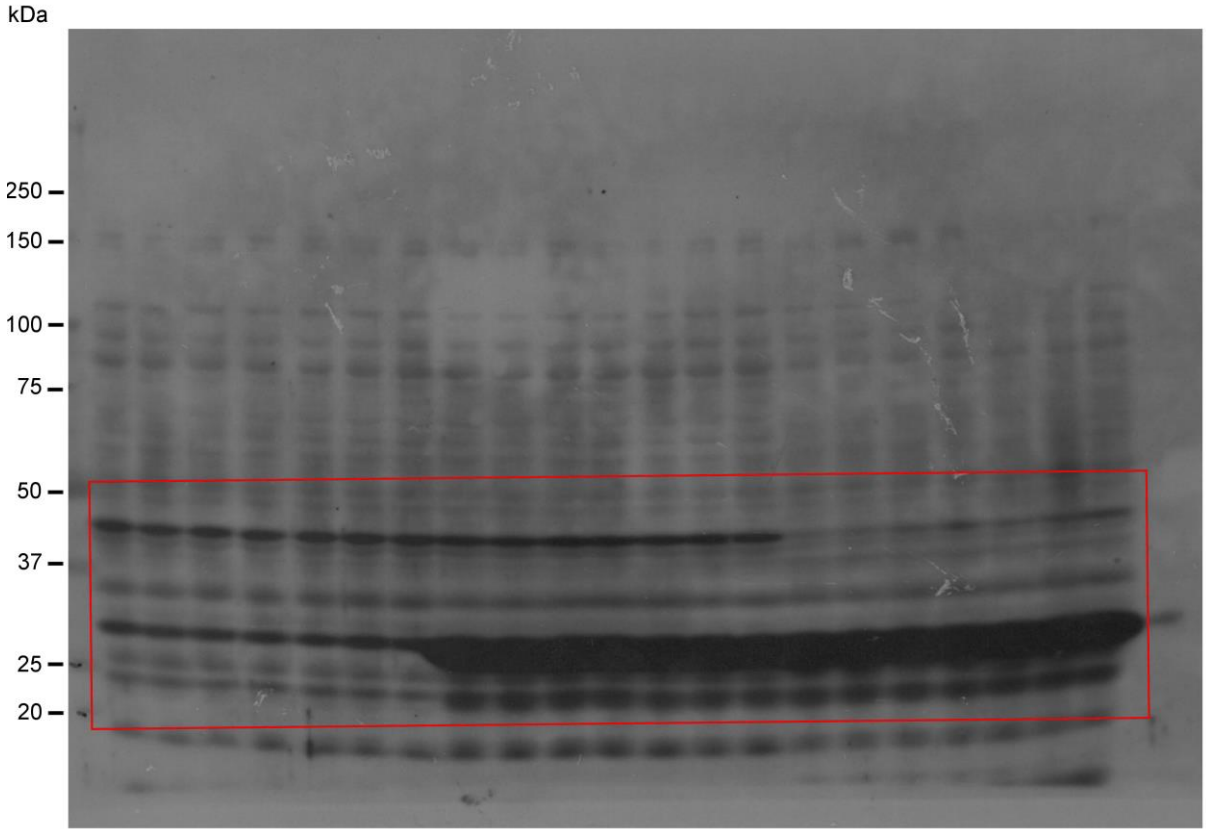

Supplementary Figure 1b (left panel)

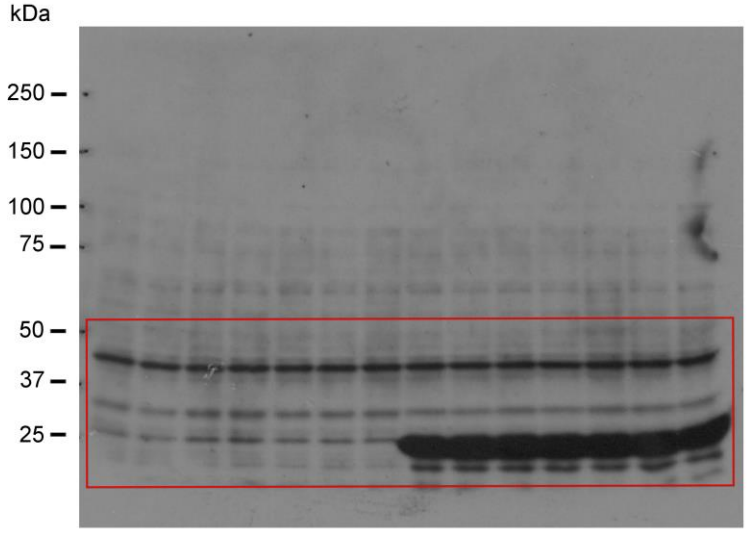

Supplementary Figure 1b (right panel)

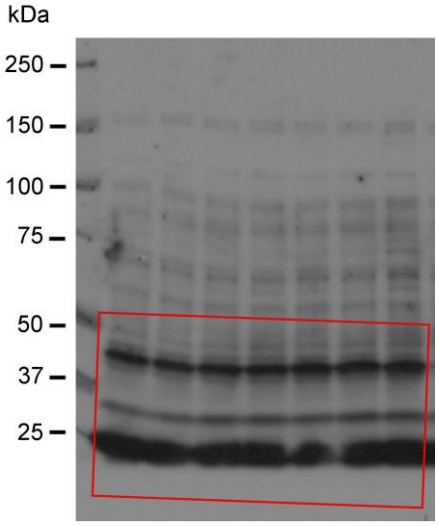

Supplementary Figure 2b Pet

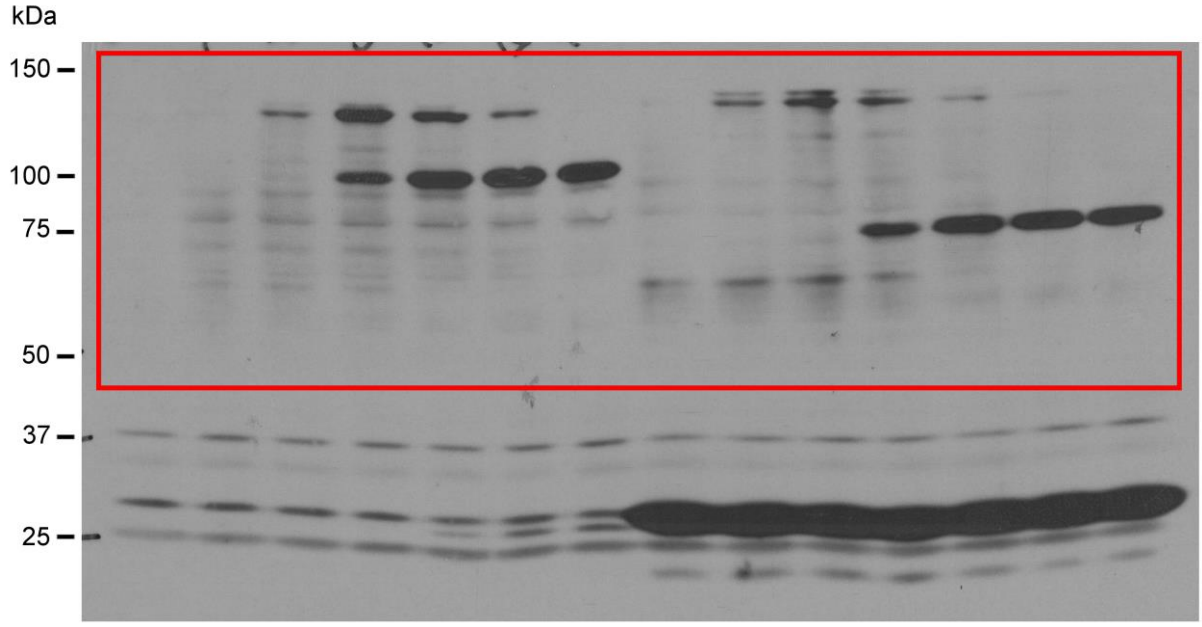

Supplementary Figure 2b PetΔL3

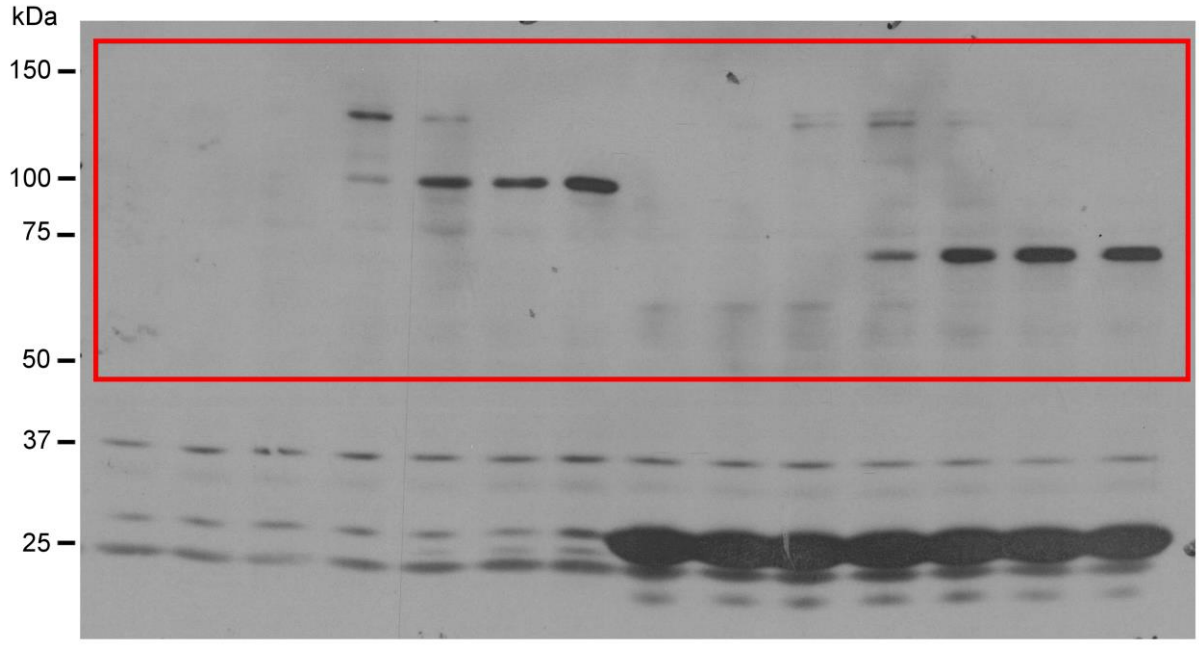

Supplementary Figure 2b PetΔL4

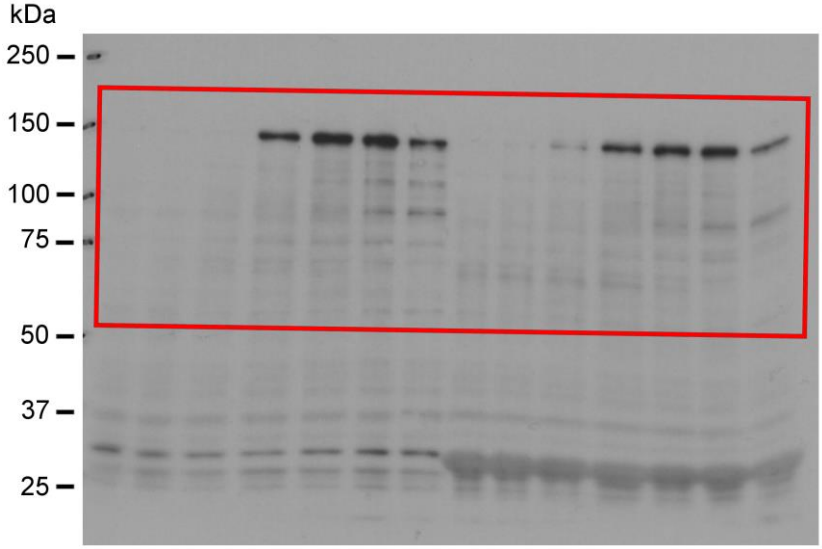

Supplementary Figure 2c PetΔL4

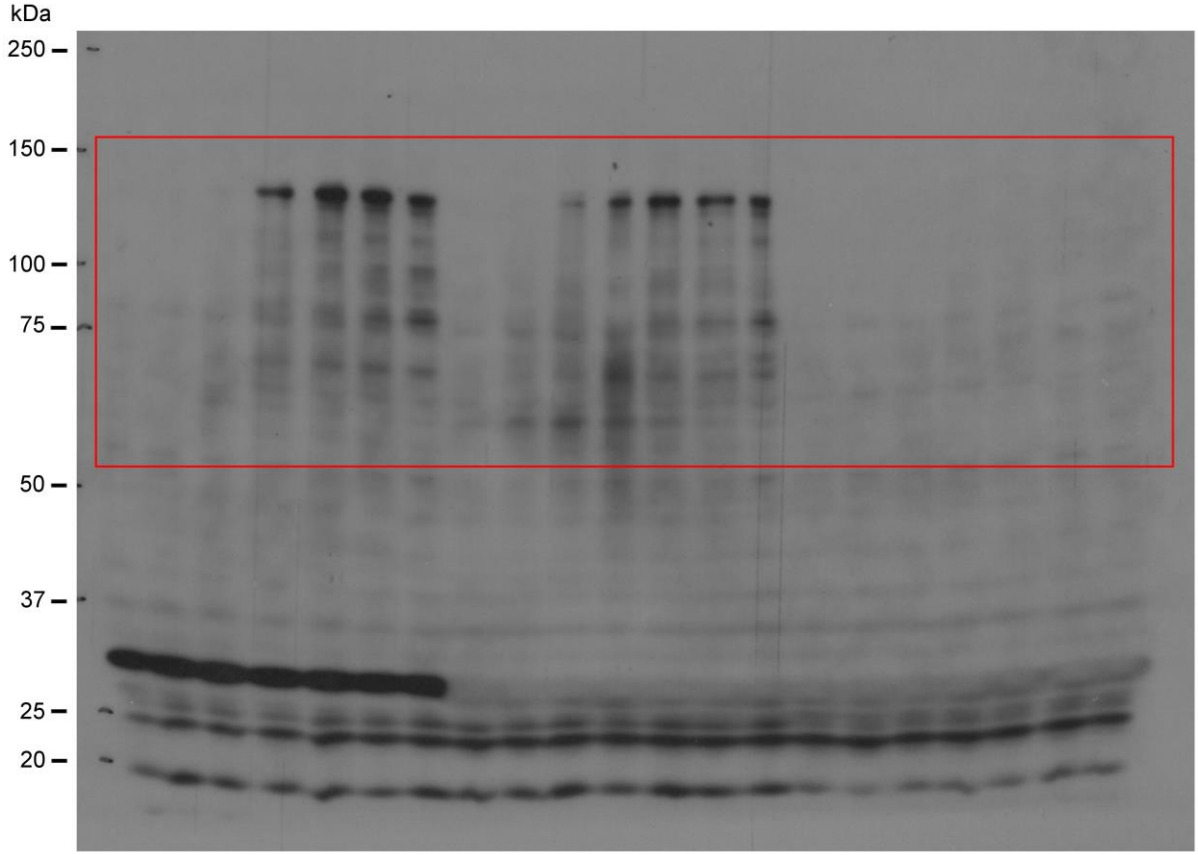

Supplementary Figure 2e Pet

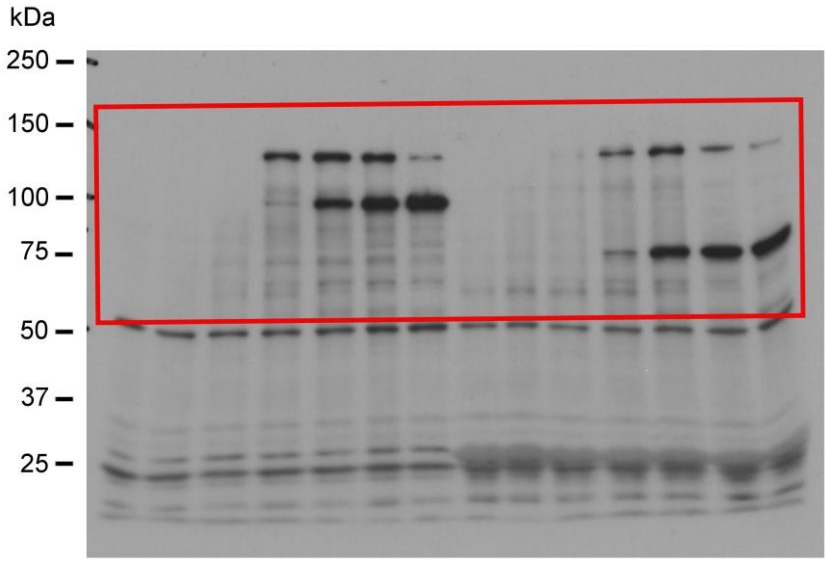

Supplementary Figure 2e PetΔL4

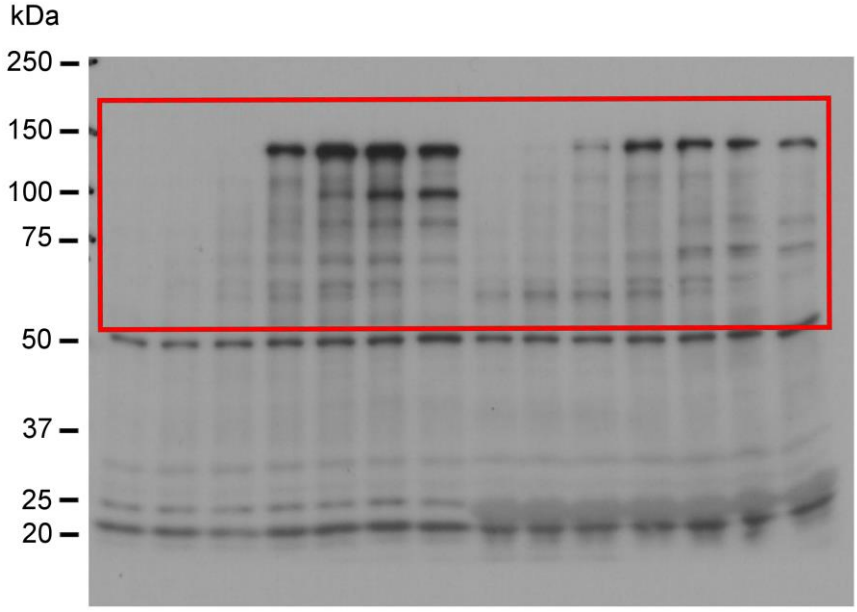

Supplementary Figure 2g Pet

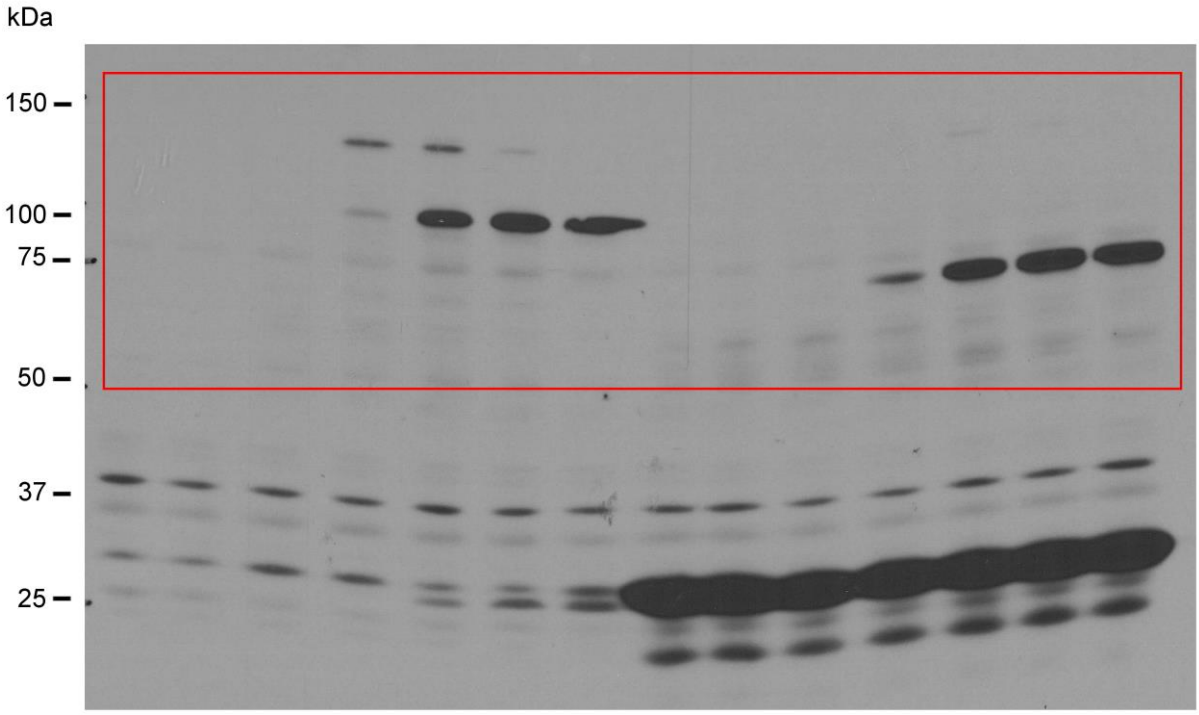

Supplementary Figure 2g PetΔL4P

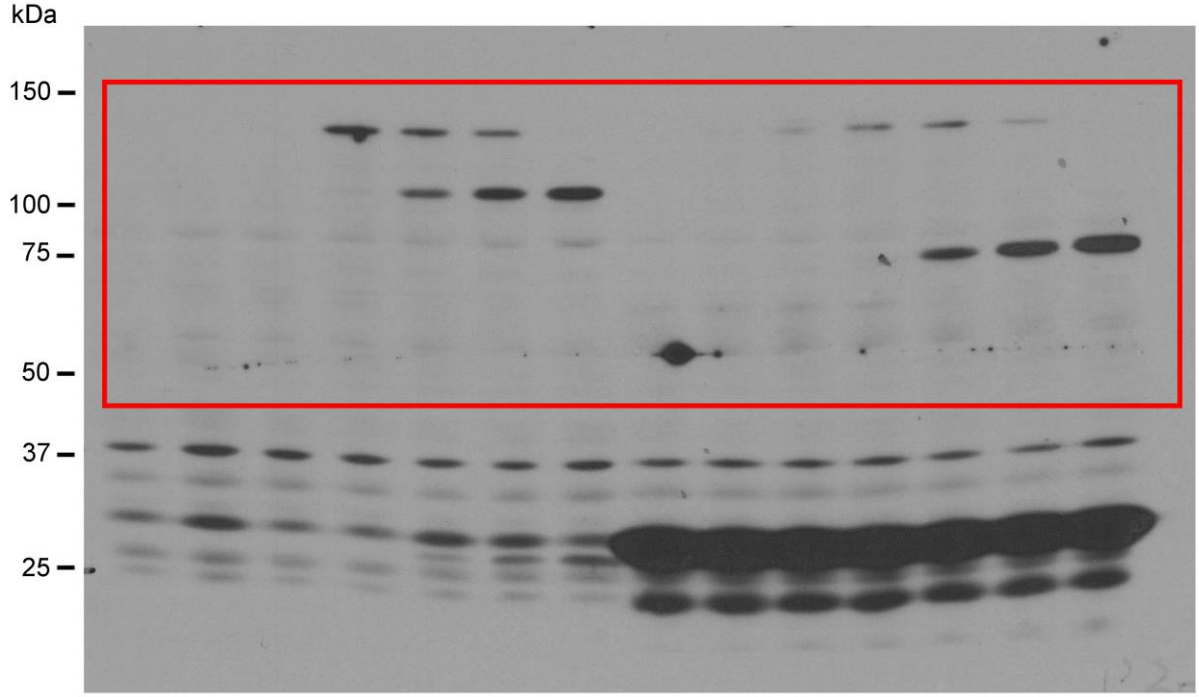

Supplementary Figure 3 Pet

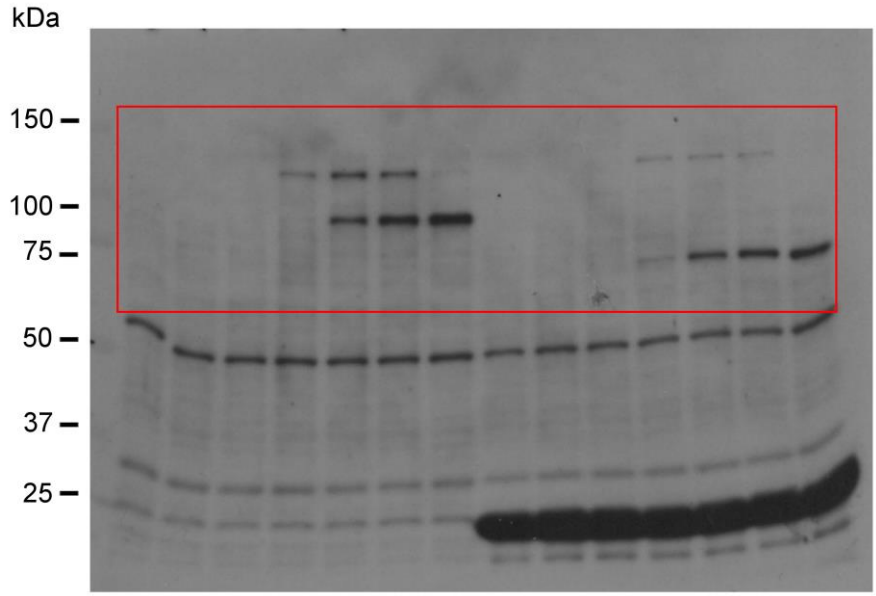

Supplementary Figure 3 PetΔL5

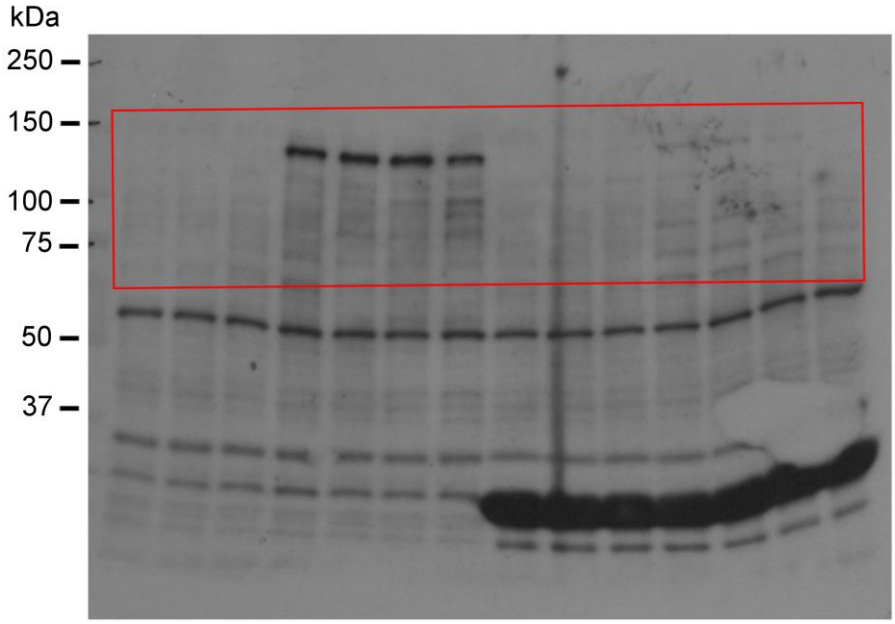

Supplementary Figure 4b Pet

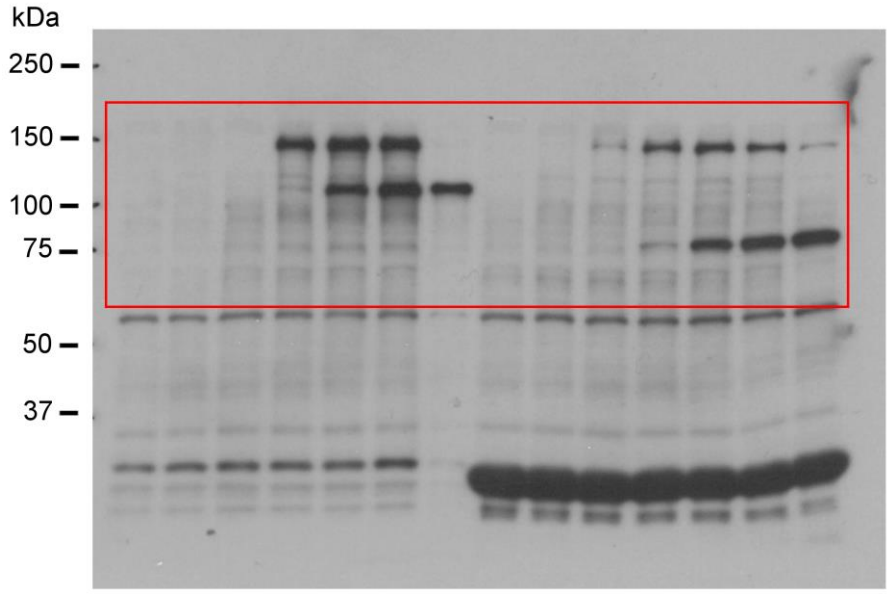

Supplementary Figure 4b PetL5β1/G

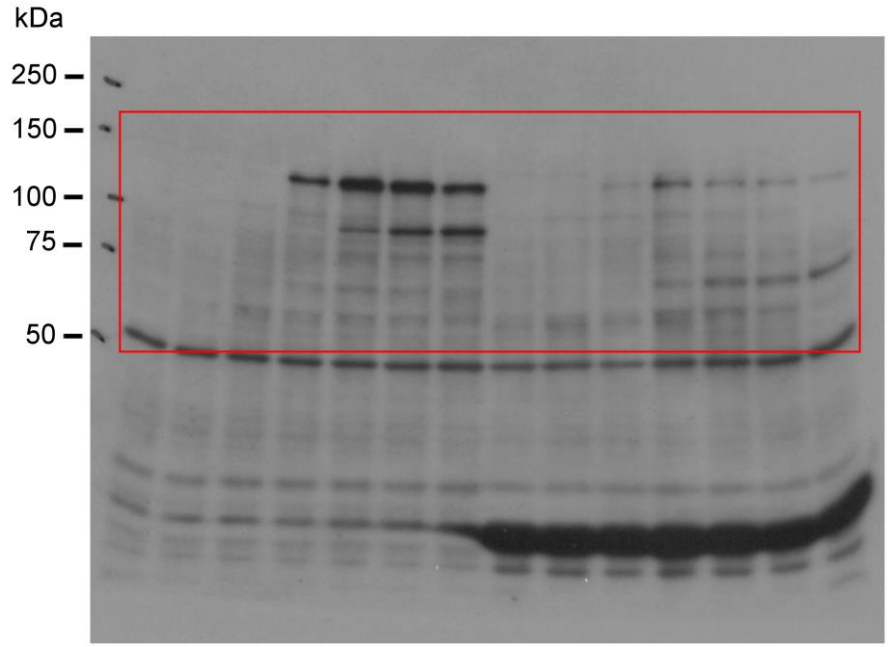

Supplementary Figure 4b PetL5β1/P

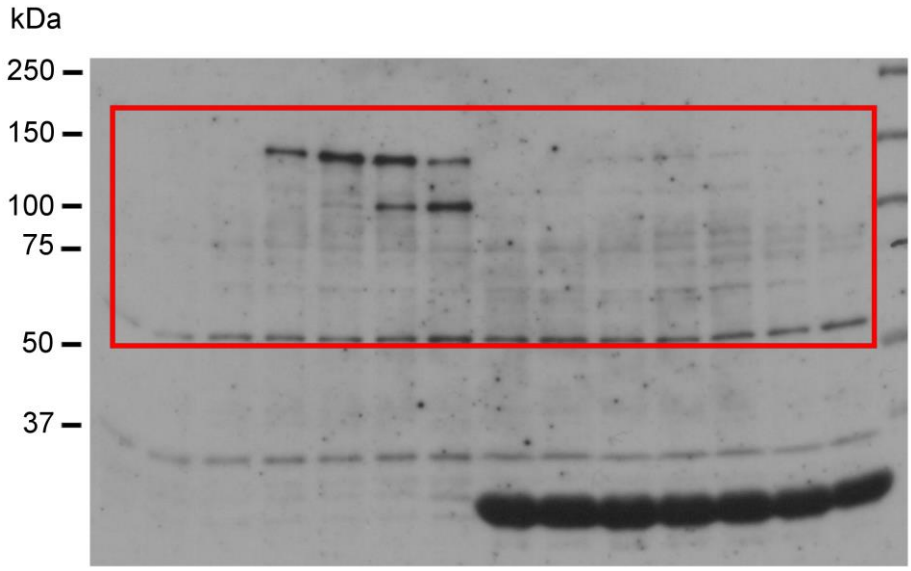

Supplementary Figure 4b PetL5OmpF

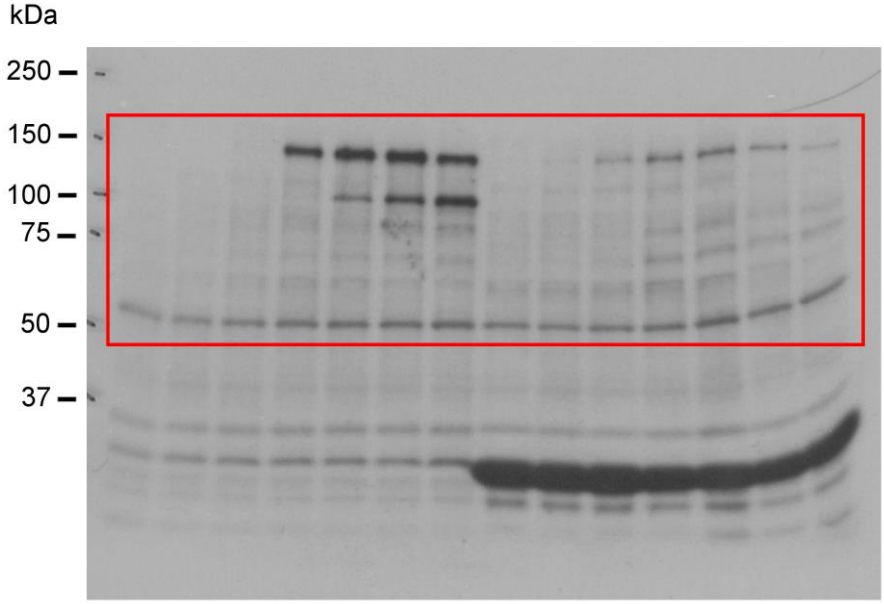

Supplementary Figure 5b Pet

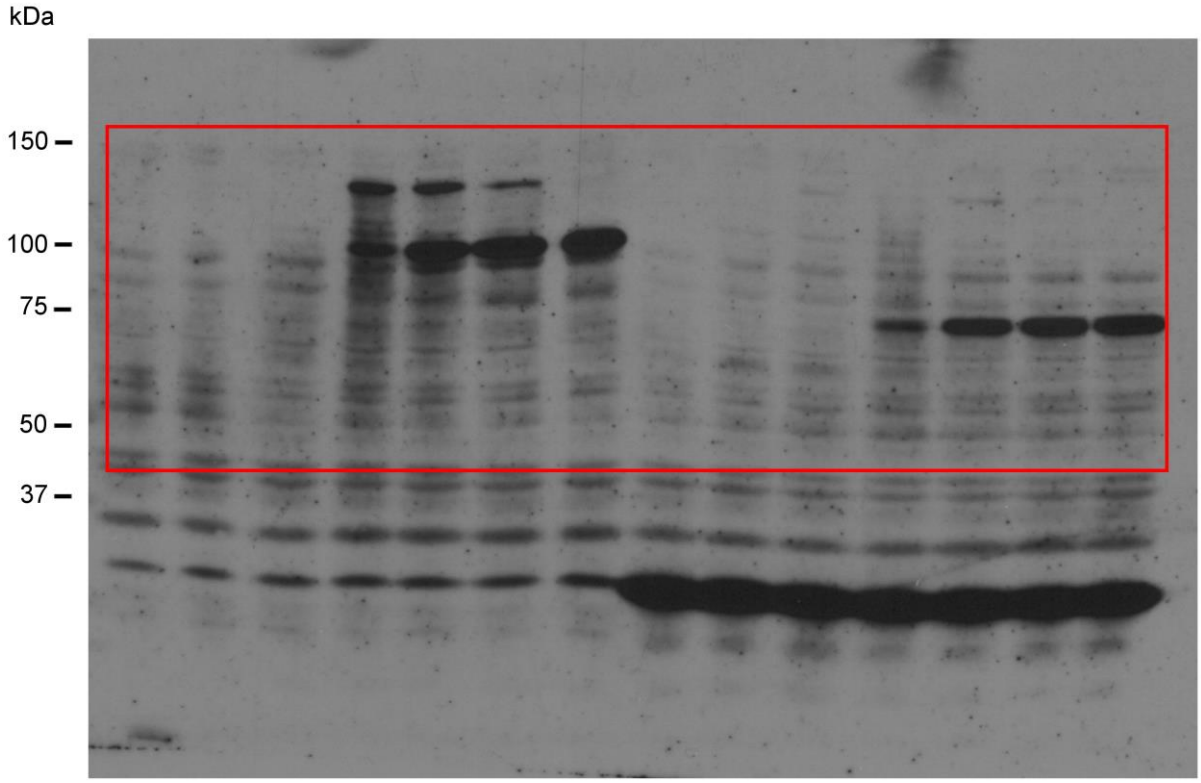

Supplementary Figure 5b PetL5VLI/N

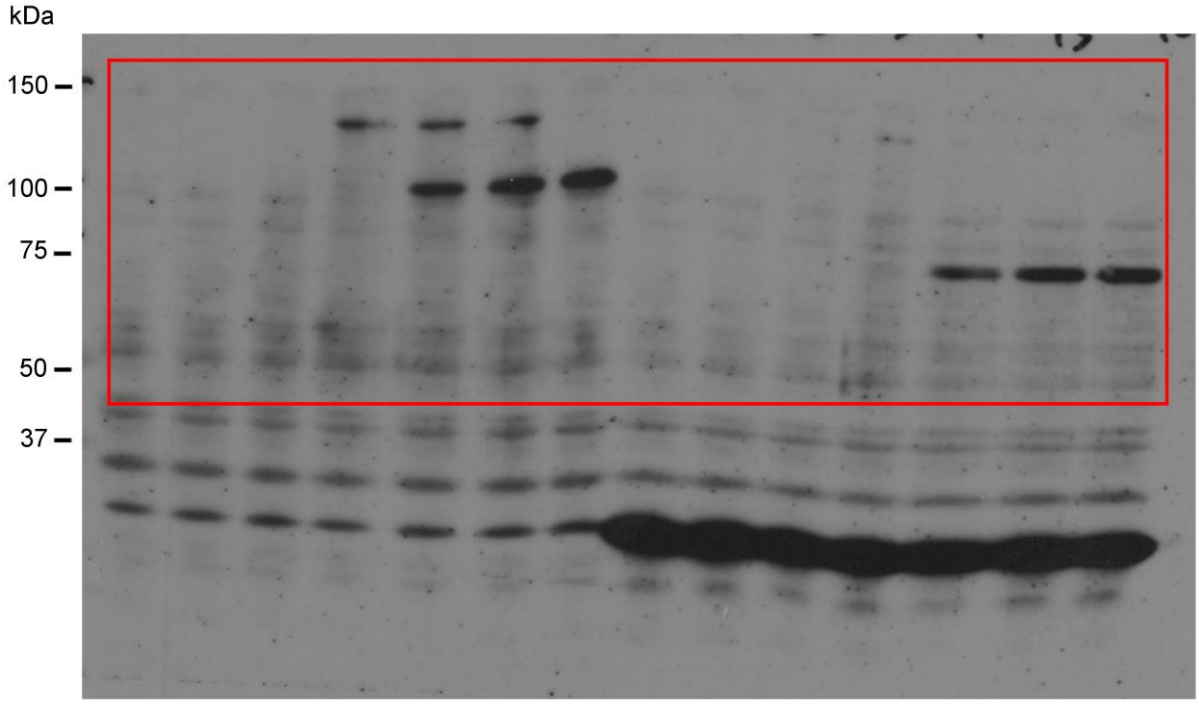

Supplementary Figure 5b PetL5R/D,E/K

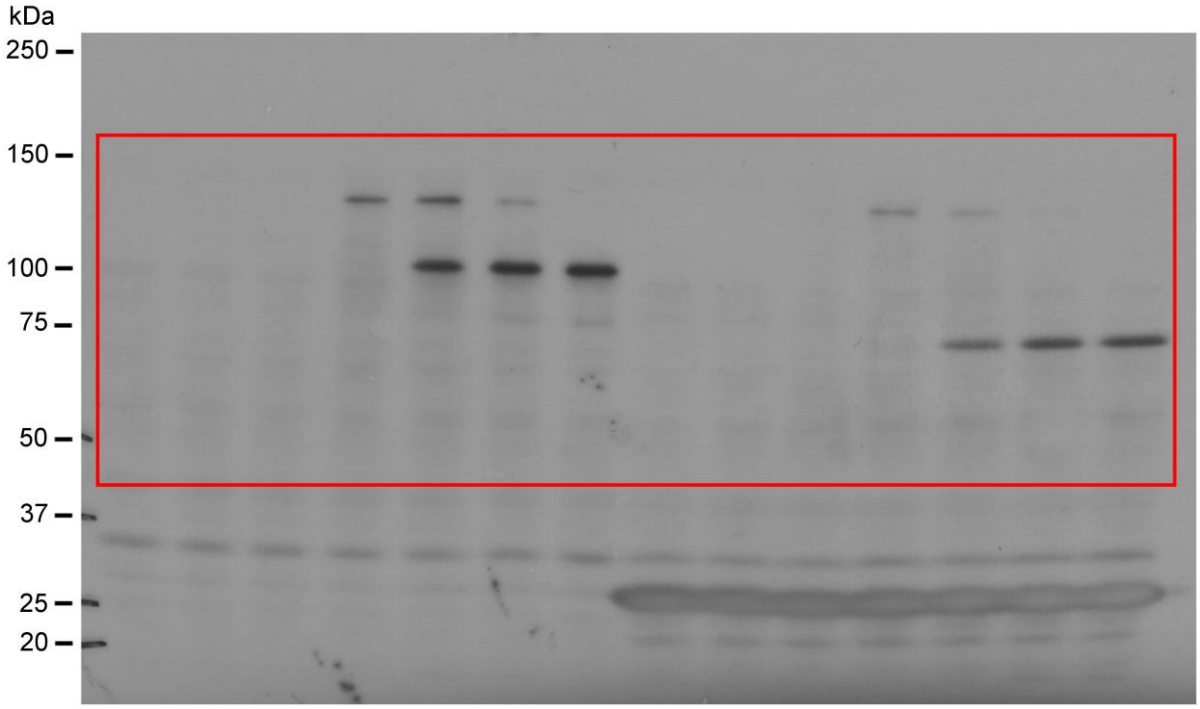

Supplementary Figure 5b PetL5TD/A

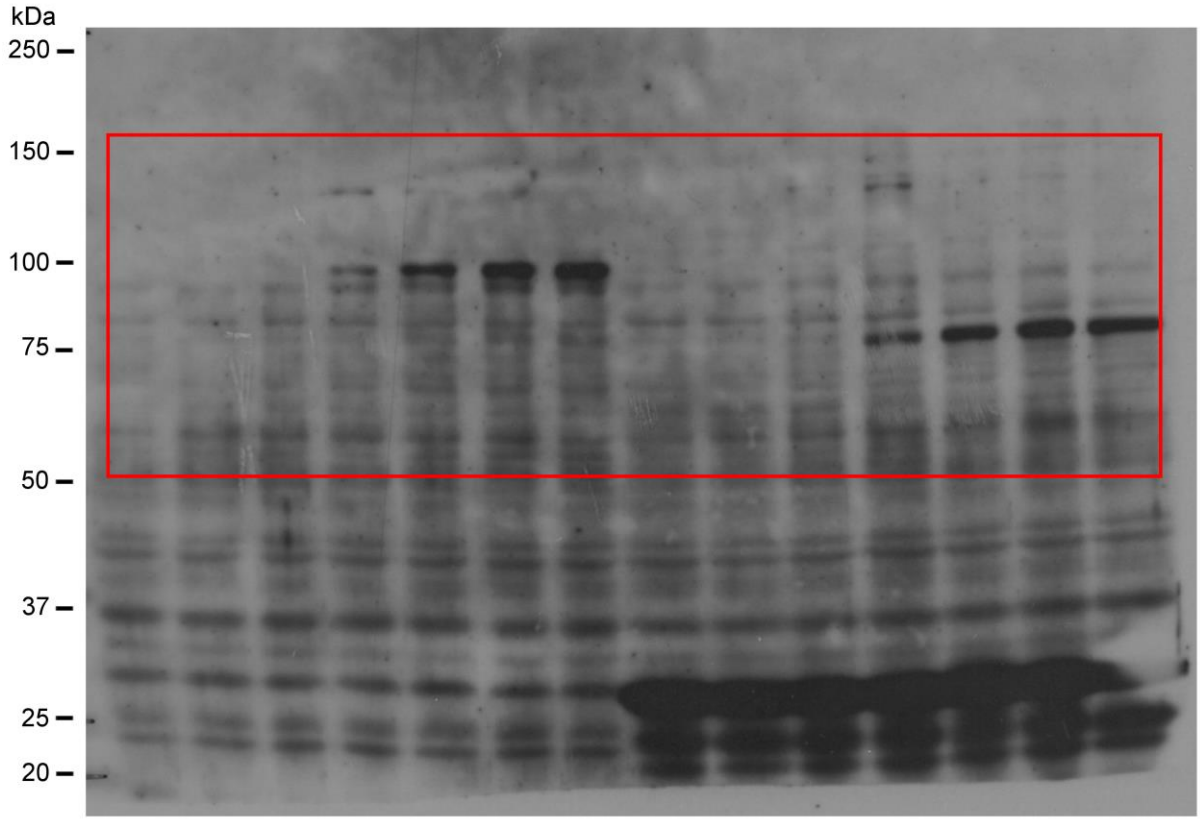

Supplementary Figure 7d Pet

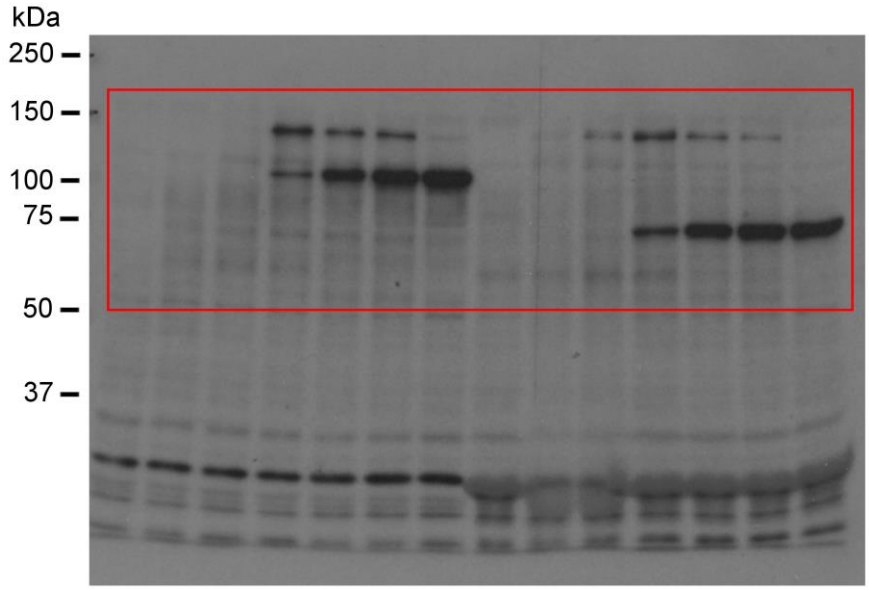

Supplementary Figure 7d PetL5AIDA-I

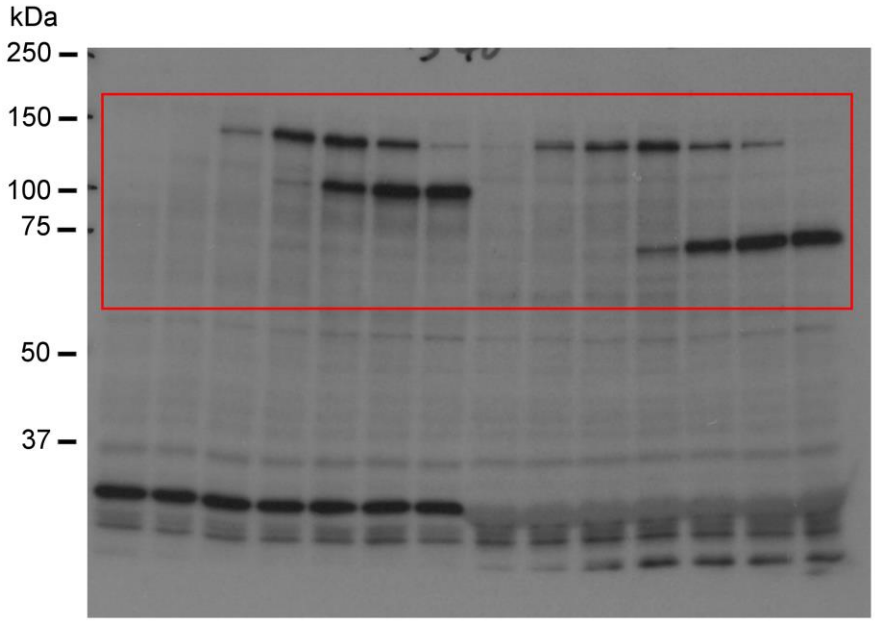

Supplementary Figure 7d PetL5EstA

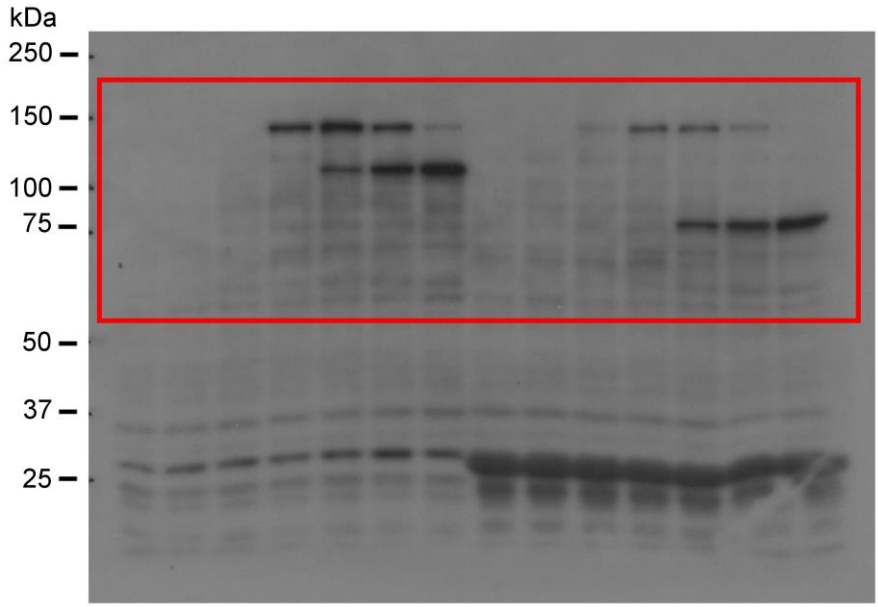

Supplementary Figure 8a PetΔ1-554 (left) **PetΔL5Δ1-554 (right)**

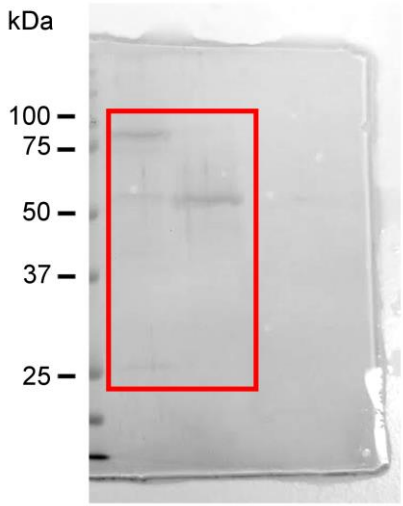

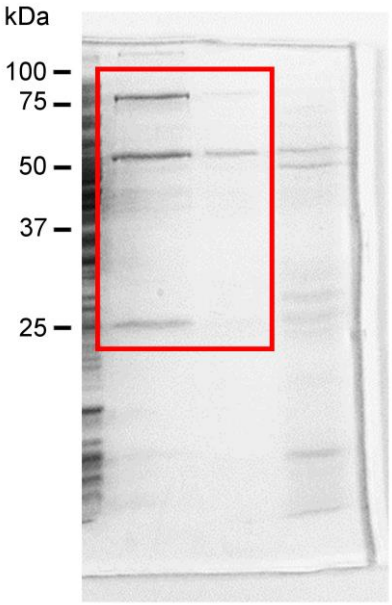

Supplementary Figure 8b PetΔ1-554 (left)

Refold IMAC

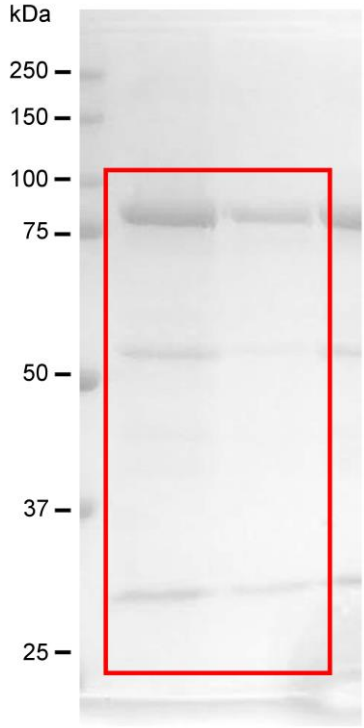

Purified β-Barrel

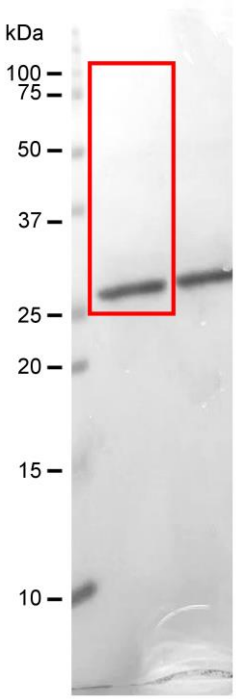

Supplementary Figure 8b PetΔL5Δ1-554 (right)

Refold IMAC

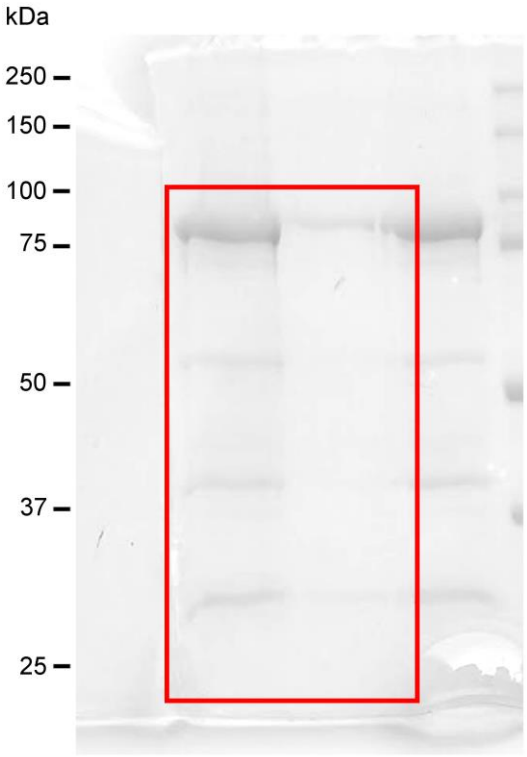

Purified β-Barrel

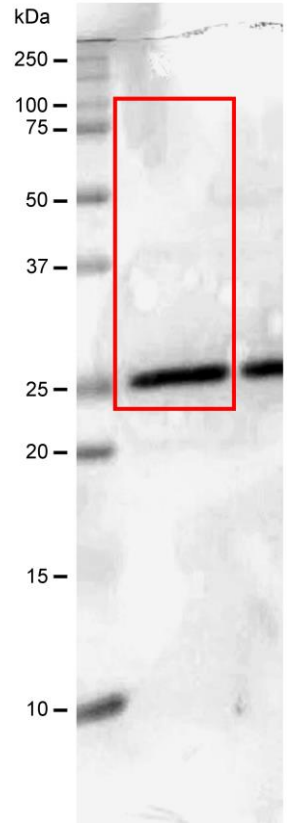

Supplementary Figure 9 | Raw image files. The raw image files of the cropped immunoblots and Coomassie-stained gels displayed in the Figures and Supplementary Figures. Sizes (in kDa) are indicated on the left. A red box is used to indicate the portion of the raw image that was cropped and displayed in the indicated Figures and Supplementary Figures.

Supplementary Table 1. Strains and plasmids used in this study

Strain/Plasmid	Relevant description	Reference
E. coli TOP10	F– *mcr*A Δ(*mrr-hsd*RMS-*mcr*BC) Φ80*lacZ*ΔM15 Δ*lac*X74 *rec*A1 *ara*D139 Δ(*ara leu*) 7697 *gal*U *gal*K *rps*L (StrR) *end*A1 *nup*G	Invitrogen
E. coli BW25113	*lacI*^{q} *rrnB*$_{T14}$ Δ*lacZ*$_{WJ16}$ *hsdR514* Δ*araBAD*$_{AH33}$ Δ*rhaBAD*$_{LD78}$	[2]
E. coli BW25113 *ompT*::*kan*	An in-frame *ompT* knock-out mutant of *E. coli* BW25113	[2]
E. coli BL21 (DE3)	F– *omp*T *hsd*SB(rB–, mB–) *gal dcm* (DE3)	Invitrogen
pBADHisA	Arabinose-inducible expression vector, ampicillin resistant	Invitrogen
pBADPet	pBADHisA derivative expressing *de novo* synthesized Pet	[3]
pBADPetΔL3	pBADPet derivative containing a *de novo* synthesized NgoMIV-AatII fragment that contains three G residues between A_{1129} and T_{1136} to express Pet with a L3 truncation	GenScript / This study
pBADPetΔL4	pBADPet derivative containing a *de novo* synthesized NgoMIV-AatII fragment that contains three G residues between K_{1176} and K_{1192} to express Pet with a full L4 truncation	GenScript / This study
pBADPetΔL4P	pBADPet derivative containing a *de novo* synthesized NgoMIV-AatII fragment that contains three G residues between F_{1178} and M_{1189} to express Pet with a partial L4 truncation	GenScript / This study
pBADPetΔL5	pBADPet derivative containing a *de novo* synthesized KpnI-EcoRI fragment that contains three G residues between N_{1231} and E_{1248} to express Pet with a L5 truncation	GenScript / This study
pBADPet$^{L5\beta1/G}$	pBADPet derivative containing a *de novo* synthesized AatII-EcoRI fragment where E_{1233}, T_{1234}, V_{1235}, L_{1236}, R_{1237}, D_{1238} in β-strand 1 of L5 are mutated to G to assess if these residues play a role in passenger domain folding	GenScript / This study
pBADPet$^{L5\beta2/G}$	pBADPet derivative containing a *de novo* synthesized AatII-EcoRI fragment where E_{1242}, K_{1243}, R_{1244}, I_{1245}, K_{1246} in β-strand 2 of L5 are mutated to G to assess if these residues play a role in passenger domain folding	GenScript / This study
pBADPet$^{L5Un/G}$	pBADPet derivative containing a *de novo* synthesized AatII-EcoRI fragment where L_{1228}, F_{1229}, A_{1230}, N_{1231}, E_{1248}, K_{1249}, D_{1250} in the unstructured region beneath β-strands 1 and 2 of L5 are mutated to G to assess if these residues play a role in passenger domain folding	GenScript / This study
pBADPet$^{L5VLI/N}$	pBADPet derivative containing a *de novo* synthesized AatII-EcoRI fragment where V_{1235}, L_{1236}, I_{1245} in β-strands 1 and 2 of L5 are mutated to N to assess if hydrophobic residues within L5 play a role in passenger domain folding	GenScript / This study
pBADPet$^{L5R/D,E/K}$	pBADPet derivative containing a *de novo* synthesized AatII-EcoRI fragment where R_{1237} and E_{1233} in β-strand 1 of L5 are mutated to D and K, respectively to disturb the putative salt bridges between R_{1237} and E_{1242}, and E_{1233} and R_{1244}	GenScript / This study

pBADPet$^{L5TD/A}$	pBADPet derivative containing a *de novo* synthesized AatII-EcoRI fragment where T_{1234} and D_{1238} in β-strand 1 of L5 are mutated to A to assess if these residues within L5 play a role in passenger domain folding	GenScript / This study
pBADPet^{L5FadL}	pBADPet derivative containing a *de novo* synthesized AatII-EcoRI fragment where β-strands 1 and 2 of L5 are replaced with a loop region from FadL (PDB 3DWO) that forms a β-hairpin structure to assess if a β-hairpin of an unrelated OMP supports passenger domain folding	GenScript / This study
pBADPet^{L5OmpF}	pBADPet derivative containing a *de novo* synthesized AatII-EcoRI fragment where β-strands 1 and 2 of L5 are replaced with a loop region from OmpF (PDB 2ZFG) that forms a β-hairpin structure to assess if a β-hairpin of an unrelated OMP supports passenger domain folding	GenScript / This study
pBADPet$^{L5β1/P}$	pBADPet derivative where E_{1233}, T_{1234}, V_{1235}, L_{1236}, R_{1237}, D_{1238} in β-strand 1 of L5 are mutated to P to eliminate potential hydrogen bonds for β-strand augmentation	This study
pBADPet$^{L5/5aa}$	pBADPet derivative containing a *de novo* synthesized AatII-EcoRI fragment where the 6-residue long β-strands were shortened to 5 residues	GenScript / This study
pBADPet$^{L5/4aa}$	pBADPet derivative containing a *de novo* synthesized AatII-EcoRI fragment where the 6-residue long β-strands were shortened to 4 residues	GenScript / This study
pBADPet$^{L5/3aa}$	pBADPet derivative containing a *de novo* synthesized AatII-EcoRI fragment where the 6-residue long β-strands were shortened to 3 residues	GenScript / This study
pBADPet$^{L5/2aa}$	pBADPet derivative containing a *de novo* synthesized AatII-EcoRI fragment where the 6-residue long β-strands were shortened to 2 residues	GenScript / This study
pBADPet$^{L5/1aa}$	pBADPet derivative containing a *de novo* synthesized AatII-EcoRI fragment where the 6-residue long β-strands were shortened to 1 residue	GenScript / This study
pBADPet^{L5EstA}	pBADPet derivative containing a *de novo* synthesized AatII-EcoRI fragment where β-strands 1 and 2 of L5 are replaced with a loop region from EstA (PDB 3KVN) that forms a β-hairpin structure to assess if the L5 β-hairpin of a non-SPATE autotransporter supports passenger domain folding	GenScript / This study
pBADPet$^{L5AIDA-I}$	pBADPet derivative containing a *de novo* synthesized AatII-EcoRI fragment where the L5 β-hairpin is replaced with a loop region from AIDA-I (PDB 4MEE) that forms a β-hairpin structure to assess if the L5 β-hairpin of a non-SPATE autotransporter supports passenger domain folding	GenScript / This study
pBADEspP	pBADHisA derivative expressing *de novo* synthesized EspP	GenScript / This study
pBADEspPΔL5	pBADPet derivative containing a *de novo* synthesized SalI-HindIII fragment that contains three G residues between N_{1236} and E_{1253} to express EspP with a L5 truncation	GenScript / This study
pET-22b+	IPTG-inducible expression vector allowing a C-terminal hexahistidine-tag fusion, ampicillin resistant	Novagen

pETPet$^{\Delta 1\text{-}554}$	Truncated pBADPet derivative containing a hexahistidine-tagged Pet barrel-domain and the last 464 residues of the Pet passenger domain	This study
pETPetΔL5$^{\Delta 1\text{-}554}$	Truncated pBADPetΔL5 derivative containing a hexahistidine-tagged Pet barrel-domain and the last 464 residues of the Pet passenger domain	This study

Note that the numbers next to the amino acid residues correspond to their position relative to the full-length Pet protein (from M^1 to F^{1295}) and full-length EspP protein (from M^1 to F^{1300}).

Supplementary Table 2. Primers used in this study

Primer	Sequence	Reference
NdeIPet464Fw	5'-GGGAATTC**CATATG**CAGGCGAACTCTATCTCT-3'	This study
XhoIPetRv	5'-CCG**CTCGAG***AGAGCC*GAAAGAGTAACGGAAGTTC-3'	[3]
SalIPetFw	5'-GCTG**GTCGAC**TTCATCGAAAAAAAAGG-3'	This study
HindIIIPetRv	5'-CAGCC**AAGCTT**TTATCAATGATGATGAT-3'	This study
MPL5β1Pro	5'-TTCGACCTGTTCGCTAACGGTCCGCCACCTCCGCC ACCGGCTTCTGGTGAAAAACGTATC-3'	This study

Restriction enzyme sequences are in bold font, insertion sequences (Gly-Ser linker) are italicized, and site-directed mutations are underlined.

Supplementary References

1. Edgar, R.C. MUSCLE: multiple sequence alignment with high accuracy and high throughput. *Nucleic Acids Res.* **32**, 1792-1797 (2004).
2. Baba, T. et al. Construction of *Escherichia coli* K-12 in-frame, single-gene knockout mutants: the Keio collection. *Mol Syst Biol* **2**(2006).
3. Leyton, D.L. et al. A mortise–tenon joint in the transmembrane domain modulates autotransporter assembly into bacterial outer membranes. *Nat Commun* **5**(2014).